Surface-Initiated Anionic Polymerization from Nanomaterials

Zhong Li and Durairaj Baskaran

Abstract Surface-initiated anionic polymerization is one of the many techniques used for the modification of organic and inorganic nanomaterials. Surface modification of nanomaterials using polymers is a unique way to reduce interface incompatibility of nanomaterials for applications in new technologies. The properties of nanomaterials strongly depend on their compatibility with organic phases either in bulk or in solution. This chapter focuses on surface grafting of polymers using living anionic polymerization from various nanomaterials and provides accounts on the developments in this area.

Keywords Surface-initiated polymerization • Carbon nanotubes • Graphene • "Grafting-from" • Anionic polymerization

1 Introduction

Unique polymers that are suitable for tailor-made applications in chemical, mechanical, and biomedical engineering are in high demand. Ultrahigh-strength polymeric materials and functional polymers that can reduce interfacial energy with other incompatible organic and inorganic materials are crucial in the development of efficient electronic devices and nanocomposites. Enhancement of strength in polymeric materials is often accomplished by blending with organic and inorganic fillers to form nanocomposites.

Since the establishment of polymer chemistry by Hermann Staudinger in the early twentieth century, polymer-based nanocomposites have been extensively studied and applied in usage to reshape modern civilization [1–3]. Nature is a great inspiration and exhibits unique composite structures everywhere [4, 5]. The development of polymer-reinforced porous ceramics is one such an example, which mimics the structural details of seashells [4, 5].

Nanocomposites based on modern carbon allotropes, such as carbon nanotubes, graphene, and graphene oxide, with polymers are expected to produce ultrahigh-

Z. Li • D. Baskaran (✉)
EMD Performance Materials Corp., 70 Meister Avenue, Somerville, NJ 08876, USA
e-mail: zhong.li@emdgroup.com; durairaj.baskaran@emdgroup.com

N. Hadjichristidis, A. Hirao (eds.), *Anionic Polymerization*,
DOI 10.1007/978-4-431-54186-8_11

strength and electrically conducting materials [6–8]. On the other hand, nanomaterials that are used in technologies, such as sensors, optoelectronics, and imaging, require specific functionality at their interface that is specially introduced by surface modification via covalent grafting or functionalization. Thus, polymer grafting onto the surfaces of organic and inorganic nanomaterials is very important to tailor-make materials that are suitable for niche applications.

1.1 Necessity for Surface Modification of Nanomaterials

Nanomaterials can be classified broadly into inorganic and organic, which can be further subdivided into various materials exhibiting unique dimensional, structural, and surface properties as shown in Scheme 1. The presence of polar and nonpolar secondary interactions in nanomaterials induces intermolecular interactions leading to aggregation, which prevents intermixing with polymers. Although there exist weak non-covalent interactions, including van der Waals, dipole-dipole, hydrogen bonding, CH-π, OH-π, and π-π, in between polymers and nanomaterials, they generally cannot overcome intermolecular interaction forces within the nanomaterials.

A low inherent incompatibility between organic polymers with fillers such as carbon nanotubes (CNTs), graphitic materials, and other inorganic components is due to a high interfacial energy that prohibits coexistence of these materials in a single phase [9, 10]. Thus, simply blending these nanomaterials with polymers often leads to macrophase separation and produces poor mechanical stability. To reduce interfacial energy and to improve compatibility, nanomaterials need to be surface modified. Even in the case of cross-linked polymeric nanoparticles, one has to choose a compatible polymer matrix to form nanocomposites.

Grafting technique is widely used to modify surfaces of nanomaterials and to enhance dispersion of nanomaterials in the polymer matrices. The surface of nanomaterial is, generally, grafted with compatible polymer or small molecule that reduces interfacial tension and enables dispersion in organic solvents and polymer matrices. For example, blending the clay, such as montmorillonite, into

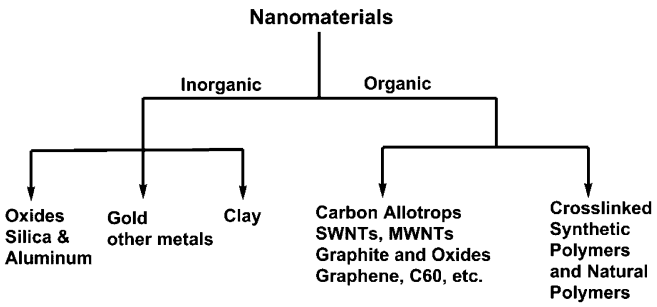

Scheme 1 Classification of nanomaterials that are used in surface-initiated anionic polymerization

a polymer can face a serious macrophase separation due to the difficulty in exfoliating the silicate layers bonded by ionic interactions. However, if montmorillonite is pretreated by intercalation of organoamines, nanoscale distribution can be achieved in polymer composites to largely enhance the mechanical properties, thermal stability, and gas barrier ability. Similar situations have also been known for CNT-based polymer composites. A strong aggregation of CNTs significantly affects the mechanical and electronic properties of the polymer composites due to inadequate tube debundling, inefficient load transfer, and limited percolation network formation. Therefore, organic and inorganic nanomaterials are, in general, require to be surface modified to improve organophilic character that suppresses aggregation and promotes molecular dispersion.

1.2 Surface-Initiated Polymerization

Several strategies have been used for the functionalization of nanomaterials through covalent and non-covalent reactions with polymers. Covalent functionalization through post chemical reactions and non-covalent functionalization through intermolecular interactions have been attempted to modify the surfaces of nanomaterials. Compared to non-covalent functionalization, which simply relies on either physisorbed or chemisorbed buffer layer to close the surface energy gap between nanomaterials and polymers, covalent chemical functionalization has been widely used to provide sophisticated surface manipulation. There are two basic functionalization strategies, namely, grafting-from and grafting-to, depending on whether the covalently attached polymer is initiated from, or performed functional polymer is reacted to the nanomaterial surfaces, respectively.

It is worth noting that the grafting ω-functionalized polymer via a grafting-to method usually is inefficient due to entropy penalty associated with the conformation of high molecular weight polymer. Thus, for grafting high molecular weight polymers, the grafting-to method is not a preferred one. The grafting-from strategy otherwise called surface-initiated polymerization (SIP) is the most promising one, since it provides a certain degree of control over polymer brush density, layer thickness, composition, and architecture of the brushes (Fig. 1). Depending on the grafting density (d), the polymer assumes different conformations, such as random-coil and extended-coil, leading to different layer or film thicknesses (LT or FT). By controlling the attachment of initiating groups on the surface and the polymerization to grow predetermined molecular weight, the surface energy can also be tuned.

The mechanism of polymer growth from solid surfaces is complex compared to the homogeneous solution polymerization and affects uniform initiation and propagation depending on the size of the surface and the interface interaction with medium of the polymerization. Thus, the reactivity, especially in the case of ionic initiators grafted at high concentration localized at the surface, may be different due to intimate ion-pair interactions leading to dormant aggregates. Moreover, the propagating centers confined in a quasi-two-dimensional area at the interface of

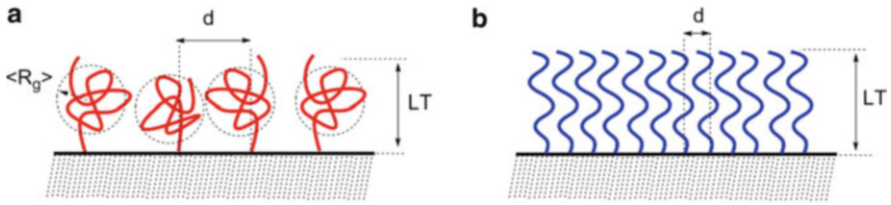

Fig. 1 Configuration of polymer brushes on surfaces with different graft density. (**a**) A low and disperse grafted brushes with coil-like conformation and (**b**) a high brush density with extended forest-like conformation

the surface to the monomer solution will change the surface properties that likely influence the monomer flux at the surface for the polymerization [11]. Therefore, the kinetic considerations are more complex and challenging to grow narrow distributed polymer chains from solid surfaces.

A successful surface-initiated polymerization involves three steps as shown in Scheme 2. An introduction of potential initiating functionality is the first step towards growing polymers from the surface of nanomaterials. The functional group is, then, activated using a catalyst or an external initiator for controlled polymerization (second-step). Subsequently, the polymerization is initiated from the nanomaterials to grow polymer brushes (third-step). Covalent attachment of the potential initiating functionality is generally performed via grafting-to method using appropriate organic reactions suitable for the chosen surface of nanomaterials. The initiators for SIP are aptly designed considering the nature and the availability of functionality on the surface of nanomaterials.

The advent of controlled or living polymerization techniques enables successful SIP from nanomaterials. In fact, the use of controlled or living polymerization is a prerequisite for grafting polymer from nanomaterials as the propagation of chains from the surfaces occurs without undergoing termination and transfer reactions. All known types of controlled and living polymerization techniques have been utilized for grafting polymers covalently from nanomaterials. Methods that have been employed are atom transfer radical polymerization (ATRP), reversible addition fragmentation chain transfer polymerization (RAFT), nitroxide-mediated radical polymerization (NMRP), living ionic polymerization, and ring-opening polymerization (ROP). Among these techniques, the living anionic polymerization provides several advantages over other methods such as control of molecular weight even at very low initiator concentration, transfer- and termination-free nature of propagation, and narrow distribution of polymer (MWD). These characteristics would allow one to control the grafting density and chain conformation of polymer brushes grown from nanomaterial surface [12]. However, the living anionic polymerization can only be performed from surfaces, which are not a deterrent to the propagation. Surfaces that contain acidic hydrogen cannot be used for surface-initiated anionic polymerization (SIAP). In this chapter, we intend to focus on the recent developments of SIAP from nanomaterials.

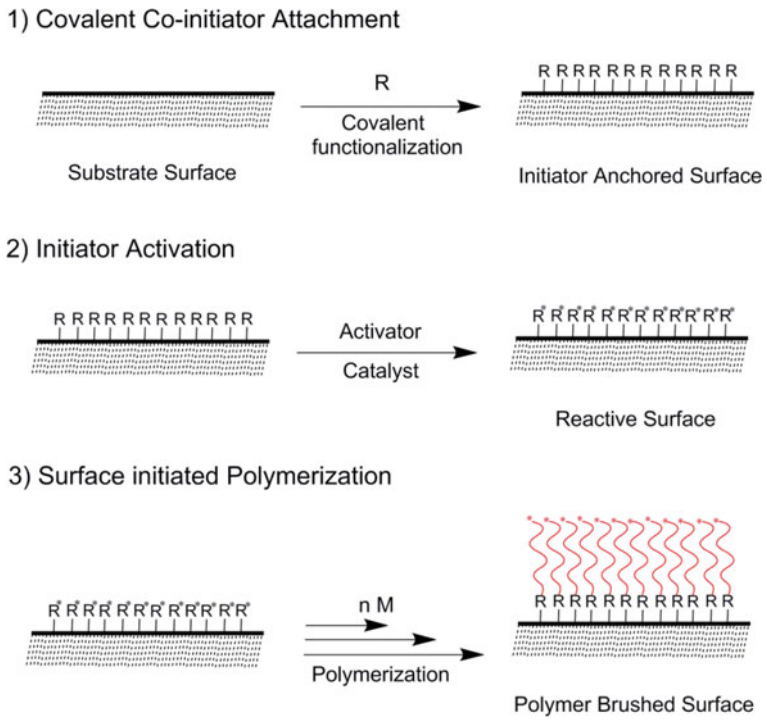

Scheme 2 Essential steps of surface-initiated anionic and other living/controlled polymerizations from theoretical surfaces of nanomaterials

2 Surface-Initiated Anionic Polymerization from Inorganic Surfaces

Inorganic materials have distinct chemical functionalities on their surfaces. They also vary in dimensions such as nanoparticles, nanoplatelets, and large flat surfaces (Scheme 3). In order to modify inorganic surfaces via SIAP, a precursor or co-initiator has to be attached on them using appropriate chemistries suitable for the surface. Specific connectivity for a particular surface, such as –S-Au– for gold, covalent –Si-O– bond for silicon wafer and silica nanoparticles, and ionic bond for layered aluminosilicates (clay), is chosen to link potential co-initiator moiety before subjecting the surface to the polymerization (Scheme 3).

Reactivity of carbanions toward the hydroxyl and carboxylic acid groups that are often found in these surfaces is very high, and hence protic functional groups have to be protected to sustain polymer growth. More importantly, the reactivity of anionic centers varies depending on the polarity of the medium in which the polymerization is conducted. Anionic polymerization in polar solvents such as tetrahydrofuran (THF) and dimethoxyethylene (DME) involves solvent-separation

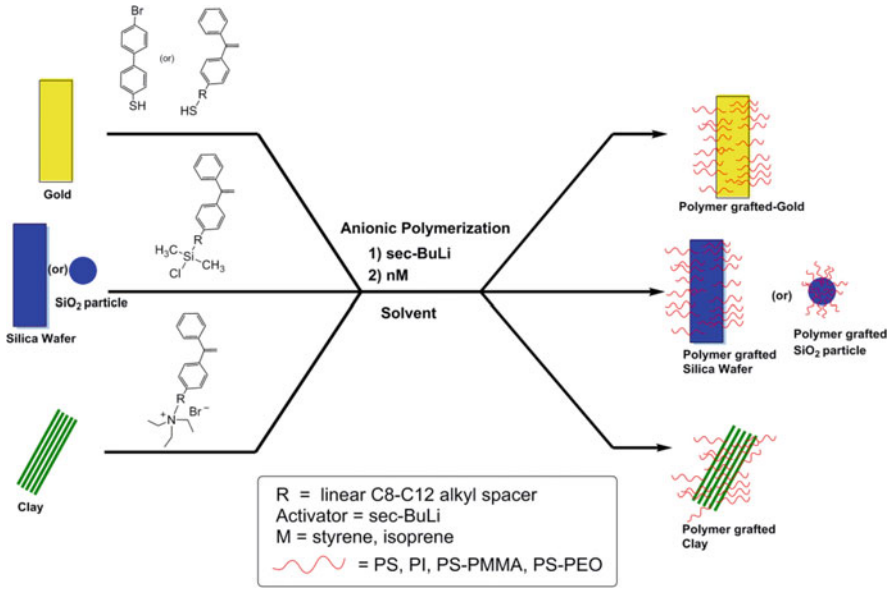

Scheme 3 Illustration of different strategies used in surface-initiated anionic polymerization from inorganic substrates

and even free ions, depending on the concentration, that are very reactive and can react with surfaces like Si-O-Si links. Thus, optimum reaction conditions should be chosen for SIAP.

Accordingly, researchers have selected 1, 1′-diphenylethylene (DPE) as a precursor co-initiator to functionalize various substrates [13–21]. The structure of DPE is unique with a sterically hindered diaryl substitution at α-carbon, and as a result, it will not undergo homopolymerization. However, the double bond of the DPE can be easily reacted by *n*- or *sec*-butyllithium (BuLi) to form an adduct with a resonance-stabilized carbanion. The resulting diphenylalkyl anion with lithium as counter cation is reactive for initiation of styrene, diene, and methacrylates [22–24]. Therefore, many of the approaches in the surface-initiated anionic polymerization involve the usage of DPE as a precursor co-initiator as shown in Scheme 3.

2.1 Anionic Polymerization from Gold Surface

It is well known that through a robust S-Au bonding, the gold surface can be easily functionalized by a self-assembled monolayer (SAM) of versatile thiol derivatives. Using S-Au bonding, a broad range of chemistries has been applied to attach precursor co-initiators on gold for surface-initiated anionic polymerization. The first example of SIAP on a flat gold surface was demonstrated by Ulman and coworkers [25]. They used 4′-bromo-4-mercaptobiphenyl thiol to functionalize

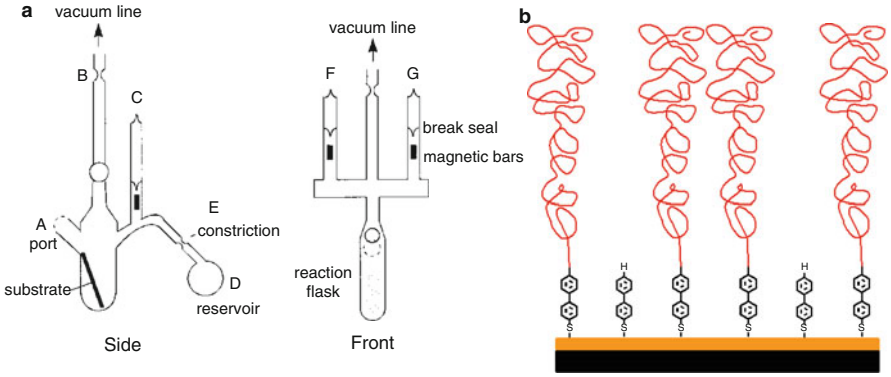

Fig. 2 (**a**) All-glass reactor used for SIAP of styrene (Reproduced with permission from Ref. [25], Copyright 1999 ACS) (**b**) The surface-induced living anionic polymerization by using the self-assembled monolayer of 4′-lithio-4-mercaptobiphenyl

the polycrystalline gold surface via SAM (Fig. 2a). The SAM-decorated gold substrate was then introduced into a sealed anhydrous reactor and reacted with *sec*-BuLi to form aryllithium initiator via halogen-metal exchange in a nonpolar medium. After a thorough washing of the aryllithium gold surface with a fresh solvent under high-vacuum condition, the monolayers of aryllithium were used to initiate styrene polymerization under vacuum (Fig. 2b).

The surface was thoroughly cleaned to remove any non-grafted polystyrene (PS) via Soxhlet extraction in toluene. The brush thickness probed by ellipsometry indicated that the PS film of 18 nm was the surface of gold in a collapsed state. It was found that the surface of the grafted PS brush contained defects such as dimples or holes corresponding to the film thickness. Upon swelling in toluene, the brush thickness increased to 29 nm. The authors used the thicknesses of the brush in the collapsed and the swollen states to estimate the degree of polymerization by applying the self-consistent mean field theory [26]. The calculated graft density based on R_g (50.6 Å) of the grafted PS chains was 7–8 chains/R_g^2, which corresponded to the area of 3.6 nm^2/chain (Table 1, entry 1) and suggested that the tethered polymer chains were adopting a stretched conformation. Although the SAM coverage indicated a dense packing of precursor mercaptobiphenyl molecules (0.2 nm^2/molecules), the numbers of grafted PS chains are relatively low, 1 in 18 molecules of SAM. This could be attributed to several factors as the efficiency of metal-halogen exchange reaction in self-assembled molecules and the reactivity of ion-pairs of the closely packed aryllithium monolayers are not known.

Advincula and coworkers later extended this technique to prepare SAM on gold using DPE-based thiol derivative as a precursor co-initiator [27]. They used *n*-BuLi to activate DPE SAMs and grafted polystyrene-*b*-poly(ethylene oxide) (PS-*b*-PEO) and polyisoprene-*b*-poly(meth methacrylate) (PI-*b*-PMMA) from gold-coated glass surface. They obtained inhomogeneous, thinner polymer brushes in the range 5–12 nm (Table 1, entry 2). One interesting aspect was to understand

Table 1 SIAP on different substrate surfaces

Entry	Type of surface	Attached initiator functionality[a]	Initiator activation[b]	Monomer[c]	Solvent/additive/temperature/time[d]	Grafted polymer	Reference
Inorganic surfaces							
1	Gold	BMBP	*sec*-BuLi	S	Cyclohexane:benzene 60:40/−/rt/3 days	3.2–3.6 nm^2/chain	[25]
2	Gold	DPE	*n*-BuLi	S	THF/−/−78 °C/12 h	–	[27]
				EO	THF/*t*-BuP4/40 °C/8 days		
				S + EO	THF/−/−78 °C/4 h, then		
				I + MMA	THF/*t*-BuP4/40 °C/8 days		
					THF/−/−78 °C/4 h, then		
					THF/DPE/−78 °C/3 h		
3	Clay	DPE	*n*-BuLi	S	Benzene/−/rt/8 h	Up to 0.81 g/g of clay	[28]
4	SiO_2 (nanoparticles or glass slide)	S	*t*-BuLi	S, 2VP, MMA, I, CMS	Homopolymers:	Up to 45 wt %	[29]
				S + I + S, S + MMA, S + 2VP	Toluene/−/rt/−		
					Block copolymers:		
					PMMA and P2VP blocks		
					Toluene/−/−80 °C/−		
					Other blocks		
					Toluene/−/rt/−		
5	SiO_2 nanoparticles	DPE	*n*-BuLi or *sec*-BuLi	S	Benzene/THF/rt/2 days	–	[30]
6	Si/SiO_2	DPE	*n*-BuLi or *sec*-BuLi	S	Benzene/THF or TMEDA or BuOLi/rt/up to 5 days	Thickness up to 23.4 nm	[31]
				S + I, BD + S	Benzene/THF or TMEDA or BuOLi/rt/1 w		

7	Si/SiO_2	DPE	*n*-BuLi	I	Benzene/−/rt/	0.10–0.24 nm^2/chain	[22][a]
				S	Benzene/−/rt/4 days	Thickness up to 24 nm	22][b]
				I + EO	Benzene/−/rt/87 + 40 h		
8	SiO_2 nanoparticles	CP-TES	*n*-BuLi	S	Cyclohexane/THF/rt/2 h	Up to 0.032 chains nm^{-2}	[32]
9	Si/SiO_2	Si-OH	MeONa	Glycidol	Methanol/−/110 °C/15 min	Thickness up to 70 nm	[33]
Organic surfaces							
10	Carbon whisker	Surface -OH	*n*-BuLi	S, MMA	Toluene/−/0 °C/1 h	39–100 wt %	[34]
11	Graphene nanoribbon	sp2 carbons	Li, Na or K	S	THF/naphthalene/−78 °C/1 d	9–22 wt %	[35]
12	Graphene oxide	Surface -OH	MDI	ε-CL	THF/50–150 °C/1 h	74 wt %	[36]
13	SWNTs	sp2 carbons	*sec*-BuLi	S	Cyclohexane/−/48 °C/2 h	10 wt %	[37]
14	SWNTs	sp2 carbons	*sec*-BuLi	*t*-BA	THF/−/−78 °C/3 h	29 wt %	[38]
				t-BA + MMA	THF/−/−78 °C/6 h	47 wt %	
15	SWNTs	sp2 carbons	Li/NH_3	MMA	NH_3/−/rt/overnight	45 wt %	[39]
16	MWNTs	DPE	*sec*-BuLi	S	Benzene/−/rt/0.75–1.5 h	86–98 wt %	[40]
				S + I	Benzene/−/rt/42 h	99 wt %	
17	SWNTs	Amino alcohol	$Sn(Oct)_2$	p-Dioxanone	Toluene/−/90 °C/72 h	40 wt %	[41]
18	MWNTs	2-azidoethanol	MeOK	Glycidol	Dioxane/−/95 °C/4 h	21–91 wt %	[42]
19	MWNTs	Surface -COOH, -OH	MeOK	Glycidol	bulk/100 °C/4 h	56 wt %	[43]
20	SWNTs	Diazonium benzyl alcohol	$Sn(Oct)_2$	ε-CL	DCB/−/130 °C/24 h	63 wt %	[44]
21	MWNTs	Glycol	$Sn(Oct)_2$	ε-CL	Bulk/120 °C/24 h	32–52 wt %	[45]
22	MWNTs	Surface -OH	$Al(CH_3)_3$	ε-CL	Toluene/−/rt/18 h	95–99 wt %	[46]

(continued)

Table 1 (continued)

Entry	Type of surface	Attached initiator functionality[a]	Initiator activation[b]	Monomer[c]	Solvent/additive/temperature/time[d]	Grafted polymer	Reference
23	MWNTs	Surface -NH2	Al $(CH_2CH_3)_3$	ε-CL	Toluene/−/40 °C/25 min	–	[47]
24	MWNTs		$Sn(Oct)_2$	ε-CL	DCB/−/130 °C/16 h	58 wt %	[48]
25	MWNTs	BCB-EO	$Sn(Oct)_2$	ε-CL	THF/−/120 °C/3 min-4 h	18–98 wt %	[49, 50]
26	MWNTs	Butanediol	$Sn(Oct)_2$	$_L$-LA	DMF/−/140 °C/2–20 h	10–35 wt %	[51]
27	MWNTs	Surface -COOH	$Sn(Oct)_2$	ε-CL	DMF/−/140 °C/2–20 h	–	[52]
28	MWNTs	Surface -COOH	$Sn(Oct)_2$	α-Chloro-ε-CL	DMF/−/140 °C/2–20 h	–	[53]
29	SWNTs	BCB-EO	$CpTiCl_3$	$_L$-LA	Toluene/−/135 °C/7.5–20 h	13–94 wt %	[54]
30	MWNTs	EG	$Sn(Oct)_2$	$_L$-LA	Bulk/−/130 °C/48 h	26–34 wt %	[55]
31	MWNTs	EG	$Sn(Oct)_2$	$_L$-LA, ε-CL	Toluene/−/130 °C/48 h	73 wt %	[56]
32	SWNTs	EDA	–	γ-BLG-NCA	DMF/−/rt/48 h	–	[57]
33	MWNTs	DAH	–	ε-Boc-$_L$-Lys-NCA	THF/−/30 °C/48 h	27–54 wt %	[58]
34	SWNTs	APA	–	γ-BLG-NCA	DMF/−/rt/48 h	41 wt %	[59]
35	SWNTs	Surface -COOH	Na	ε-CL	Bulk/−/140 °C/24 h	30 wt %	[60]
36	MWNTs	Isocyanate	Na	ε-CL	Bulk/−/170 °C/2–10 h	40–65 wt %	[61]
37	MWNTs	S + MA	NaCL	ε-CL	Bulk/−/170 °C/6 h	–	[62]
38	MWNTs	Toluene 2, 4-diisocyanate	NaCL	ε-CL	Bulk/−/160 °C/10 min	–	[63]
39	Cross-linked PS beads	BIBA	SmI_2	MMA	THF/DEPA/−78 °C/12 h	–	[64]

40	Cross-linked PS beads	BIBA	SmI_2	AMA	THF/DEPA/−78 °C/8 h	–	[65]
41	Cross-linked PS beads	BIBA	SmI_2	Hydroxyethyl methacrylate	THF/DEPA/−78 °C/48 h	–	[66]

[a]*BMBP* 4′-bromo-4-mercaptobiphenyl, *DPE* 1,1-diphenylethylene, *CP-TES* (3-chloropropyl)triethoxysilane, *BCB-EO* 4-hydroxyethyl benzocyclobutene, *EG* ethylene glycol, *EDA* ethylene diamine, *DAH* 1,6-diaminohexane, *APA* 3-azidopropan-1-amine, *MA* maleic anhydride, *BIBA* 2-bromoisobutyric acid

[b]*n-BuLi n*-butyl lithium, *sec-BuLi secondary*-butyl lithium, *t-BuLi tert*-butyl lithium, *MeONa* sodium methoxide, *MDI* 4,4′-methylenebis(phenyl isocyanate), *Sn(Oct)*$_2$ tin(II) 2-ethylhexanoate, *MeOK* potassium methoxide, *CpTiCl*$_3$ cyclopentadienyltitanium(IV) trichloride, *NaCL* ε-caprolactam sodium salt, *SmI*$_2$ samarium(II) iodide

[c]*S* styrene, *EO* ethylene oxide, *I* isoprene, *MMA* methyl methacrylate, *2VP* 2-vinylpyridine, *CMS* chloromethylstyrene, *BD* butadiene, *t-BA tert*-butyl acrylate, ε-*CL* ε-caprolactam, $_L$-*LA* $_L$-lactide, γ-*BLG-NCA* γ-benzyl-$_L$-glutamate *N*-carboxyanhydride, ε-*Boc-*$_L$*-Lys-NCA* ε-(benzyloxycarbonyl)-$_L$-lysine *N*-carboxyanhydride, *AMA* allyl methacrylate, *HEMA* hydroxyethyl methacrylate

[d]*THF* tetrahydrofuran, *TMEDA* tetramethylethylenediamine, *BuOLi* lithium *tert*-butoxide, *DCB* dichlorobenzene, *DMF* dimethylformamide, *DEPA N*,*N*-diethylphenylacetamide

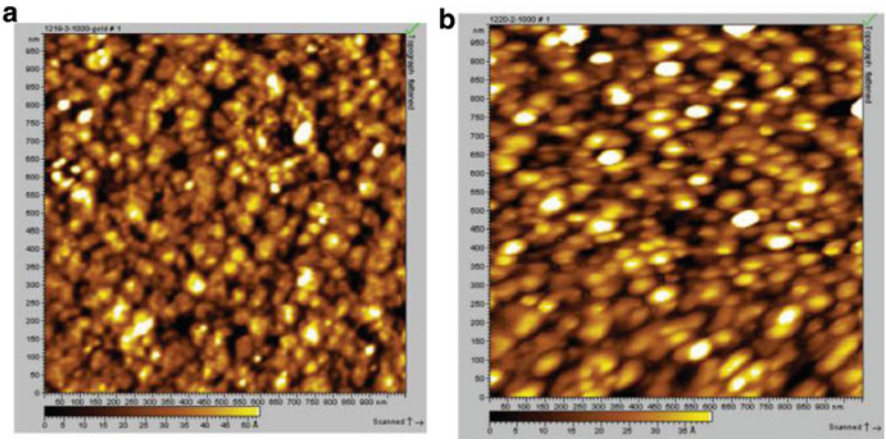

Fig. 3 (**a**) AFM images of PS-*b*-PEO diblock copolymer brush. The topological or height image before annealing. (**b**) AFM images of PS-*b*-PEO diblock copolymer brush. The topological or height image after annealing at 120 °C (Reproduced with permission from Ref. [27], Copyright 2006 Wiley)

the self-assembling behavior of the copolymer brushes. Microphase separation of the two blocks was expected; however, no self-assembling patterns were observed by atomic force microscopy (AFM) (Fig. 3), even though polymer reorganization can be induced by solvent treatment as detected by contact angle measurements. The authors attributed this observation to a small thickness of the polymer brushes and to a low molecular weight of the block segments.

2.2 Anionic Polymerization from Clay Surface

Owning to their unique layered structure and cheap availability of clays, they have been used extensively to strengthen polymer nanocomposites targeting for high thermal, environmental, and mechanical stability and to enhance the gas barrier properties. Generally, pristine clay needs to be modified by positively charged organic species via ion exchanging the metal cations like Li^+, Na^+, or Ca^{2+} in order to improve the organophilicity and to exfoliate the silicate layers for better compatibility with the polymer matrix through either a simple blending or an in situ polymerization. However, anionic polymerization involving clay is quite challenging because the hydrophilic nature of clay inevitably hosts moisture in it, which would terminate propagating living anions during grafting. As a result, reactions need to be conducted in a specially designed reactor to ensure a complete removal of moisture under high vacuum. Using high-vacuum and break-seal technique, Mays and coworkers [28] demonstrated the surface-initiated anionic polymerization of styrene from clay intercalated with DPE-functionalized triethylammonium bromide (Fig. 4).

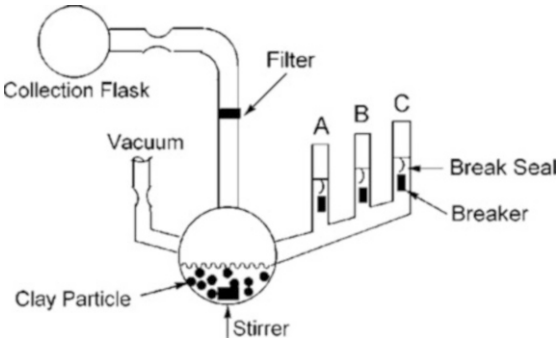

Fig. 4 Schematic diagram of the anionic polymerization reactor: (*A*) ampule containing styrene, (*B*) ampule containing *n*-BuLi, and (*C*) ampule containing MeOH (Reproduced with permission from Ref. [28], Copyright 2002 ACS)

The elegance of such a reaction setup includes a feasibility to completely remove free initiators, which is known to compete severely with the immobilized initiators for monomer consumption, as well as a direct visual monitoring of the formation of living anions bound on the substrate surface. The DPE-based initiator is thermally stable over 300 °C, which allowed the organo-modified clay free from any trapped H_2O by extensive drying in vacuum at high temperature. After treated by *n*-BuLi, the DPE carbanions were generated and, consequently, initiated the living polymerization of styrene (Scheme 3). In spite of a thorough washing of excess BuLi with the solvent, the authors found that a small amount of the free initiator is present in the polymerization solution. It is worth noting that although the SIP was confirmed by Fourier transform infrared spectroscopy (FTIR), X-ray diffraction (XRD) and X-ray photoelectron spectroscopy (XPS), the thermal gravimetric analysis (TGA) of the PS-grafted clays, the AFM imaging of the clay nanoparticles, and the polymer weight analysis of the cleaved polymer; all indicated that a significant polymerization took place only at the outer layers of the DPE-modified clay, while most of the intercalated initiators inside the gallery did not participate in the anionic polymerization. Therefore, the expected exfoliation of the clay during the polymerization was not achieved, and the grafted PS showed a much larger polydispersity index than a typical living anionic polymerization process (Table 1, entry 3).

2.3 Anionic Polymerization from Silicon Oxide Particles and Substrates

Some early works exploring the living anionic SIP on silica surfaces appeared around the 1990s. Taking advantage of the hydroxyl groups commonly existing on the SiO_2 surface, Oosterling et al. [29] developed a technology for immobilizing styrene on the silica nanoparticle surfaces using *p*-vinylbenzyltrichlorosilane. The attached styrene monomer was activated by *t*-BuLi and used for the polymerization of styrene assuming that inter-/intramolecular reactions are insignificant. Several

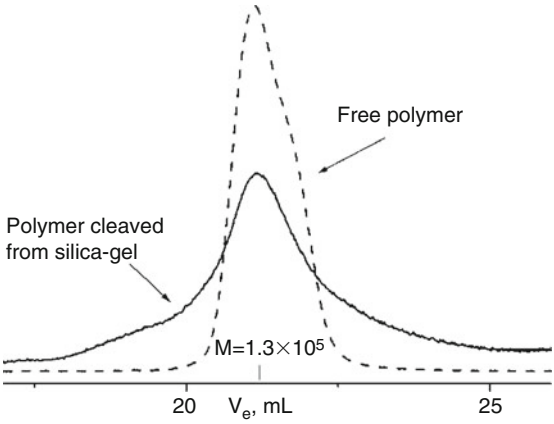

Fig. 5 Typical gel permeation chromatography results of free polymer and bound polymer cleaved from silica nanoparticles (Reproduced with permission from Ref. [30], Copyright 2002 ACS)

types of block copolymers such as PS-*b*-PI-*b*-PS, PS-*b*-PMMA, and polystyrene-b-poly(2-vinyl pyridine) (PS-*b*-PVP) were synthesized from the surface. In order to avoid a potential attack on Si-O-Si bonds by the highly reactive *t*-BuLi, the authors chose benzene as a nonpolar solvent for the polymerization. However, the molecular weight distributions were broader than the ones observed in a typical anionic polymerization, possibly due to the aggregation tendency of *t*-BuLi in hydrocarbon solvents (Table 1, entry 4).

In another study, Zhou et al. [30] connected DPE to the silica surface via silylether bond using dimethylsilylchloride-functionalized DPE. They used *n*-BuLi to activate the styrene polymerization and thus obtained PS-grafted silica nanoparticles in toluene. Although the same reactor shown in Fig. 4 was used to ensure the complete removal of nonattached free initiators through washing under vacuum, they found that some free DPE or *n*-BuLi residue was present in the polymerization solution and caused concurrent homopolymerization of styrene in small quantity. Thus, they obtained PS grafts with a broad molecular weight distribution (Fig. 5). They also reported problems associated with reproducibility and very low initiator efficiency. These results suggest that growing polymers from the silica surface is complicated due to dormancy of reaction sites, side reactions, and difficulty in the purification of surface (Table 1, entry 5).

The same group also applied the silylchloride-functionalized DPE to silicon wafer and formed SAM of DPE initiators on the surface [31]. However, a similar low grafting density was observed. On the other hand, Quirk and coworkers successfully grafted silicon wafers using both grafting-to and grafting-from approaches via anionic polymerization [22]. They used trichlorosilyl- and dimethylsilyl-substituted DPE to form SAM on the silicon wafer. The formation of a monolayer of DPE was confirmed based on the packing density (0.41 nm^2/DPE molecule) using X-ray reflectometry. The DPE monolayer was converted into 1,1-diphenylhexyllithium by reacting with *n*-BuLi and used to initiate styrene and diene monomers. The excess *n*-BuLi after activation of DPE monolayers was washed away by repeated back distillation of benzene using a high-vacuum

technique. In spite of such a treatment to remove excess *n*-BuLi from the surface, they observed 100–300 mg of free PS formed in the polymerization solution. Nevertheless, the PS grown from the silicon wafers had the highest brush thickness, 24 nm reported so far (Table 1, entry 6). The chain ends of the living polymer brushes with lithium counterion were successfully functionalized with hydroxyl group by adding ethylene oxide and further used for the polymerization of ethylene oxide in the presence of potassium counterion.

In a very recent study, Kim and coworkers applied a similar strategy to functionalize silica nanoparticles using (3-chloropropyl)triethoxysilane [32]. They used metal-halogen exchange reaction to graft PS via anionic polymerization in toluene. The efficiency of alkyl halide-metal exchange reaction with *n*-BuLi in nonpolar solvent is, in general, very low. Nevertheless, they conducted the polymerization of styrene in the presence of free *n*-BuLi and obtained two distinct components of the cleaved PS prepared by silica gel SIP (Fig. 6). The high molecular weight PS similar to the PS generated from the free initiator was attributed to grafting-to reaction of the living PS anion.

The PS brushes grown from the silica particles are distinctly different in topography as shown in the TEM images (Fig. 7). Based on the dynamic light and small angle neutron scattering studies on these silica particles, they concluded that the conformation of the grafted PS chains is "coil-like" instead of stretched or extended as expected for surface-initiated polymerization. They attributed "coil-like" brush conformation to poor grafting density (Table 1, entry 8).

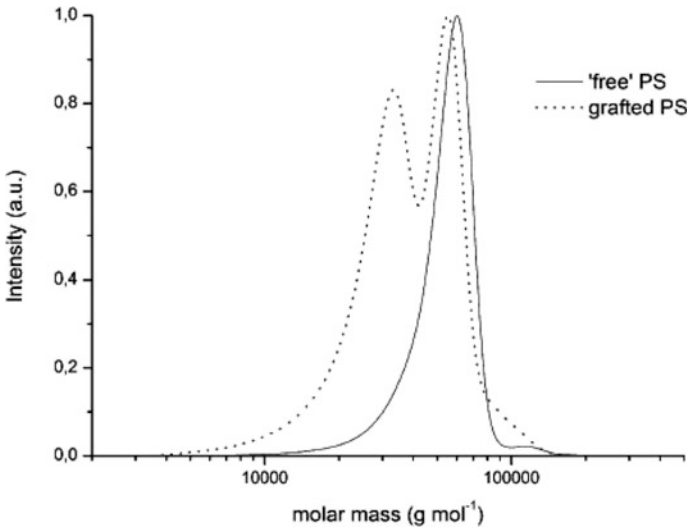

Fig. 6 GPC traces of grafted PS brushes separated from the surface and the solution. The broader bimodally distributed curves (*dotted*) correspond to the surface attached PS, which have been detached by etching. The narrow monomodal distributions (*lined*) correspond to free PS, which was initiated by sacrificial initiator in solution (Reproduced with permission from Ref. [32], Copyright 2013 Springer)

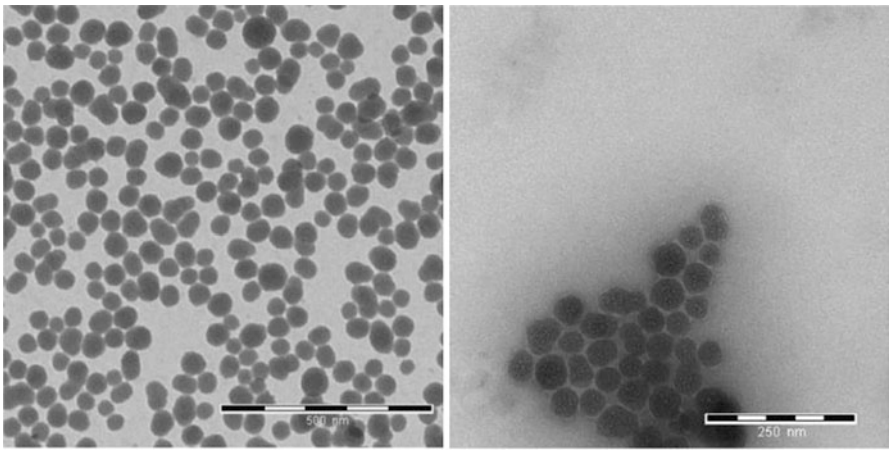

Fig. 7 TEM images of bare silica nanoparticles (*left*) and the PS-grafted silica nanoparticles (*right*) prepared by using the drop-cast method of their dispersions on carbon-coated copper grid (Reproduced with permission from Ref. [32], Copyright 2013 Springer)

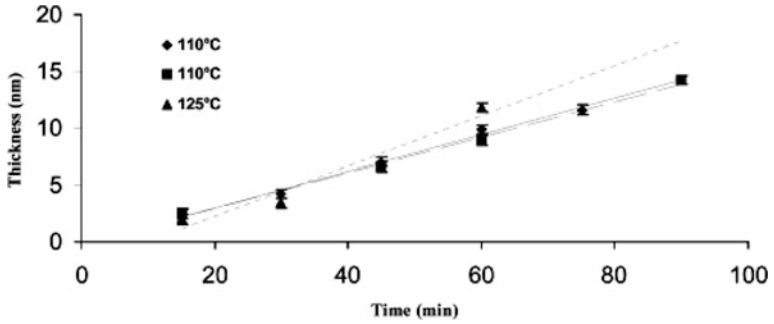

Fig. 8 Increase in polyglycidol brush thickness (measured by ellipsometry) vs polymerization time on Si wafer using various temperatures (Reproduced with permission from Ref. [33], Copyright 2003 ACS)

Other than the most studied PS grafting systems, Huck and coworkers studied the grafting of hyperbranched polyglycidol [33]. In this case, a simple deprotonation of the OH groups on the activated SiO_2 surfaces, in either Si wafer or silica gel, using sodium methoxide was shown to efficiently initiate the anionic ring-opening polymerization of glycidol. The progress of the surface-initiated polymerization was monitored, which showed clearly an increase in polyglycidol brush thickness with time (Fig. 8). Furthermore, the large amount of active OH groups on the grafted hyperbranched polyglycidol enabled them to do post-functionalization, as demonstrated by their reinitiation experiments to increase the polyglycidol brush thickness up to 70 nm (Table 1, entry 9) and the esterification of the hyperbranched polyglycidol-grafted silica gel.

3 Surface-Initiated Anionic Polymerization from Organic Surfaces

Organic substrates are broadly classified into sp^2 carbon-based nanomaterials (Scheme 4) and insoluble polymers (natural or cross-linked synthetic polymers). Depending on the nature of the functional groups present on the organic solids/surfaces, they can be used for covalent or non-covalent modifications. The non-covalent modification replies on adsorption of suitable organic molecules such as pyrenes, poly(*meta*-phenylene vinylene), poly(styrene sulfonate), cyclodextrin, etc., to form weak secondary interactions, including π-π, ionic, and H-bonding [77], and the covalent modification involves direct reactions with either the sp^2 carbons or the preexisting reactive functional groups (COOH, OH, etc.) on the substrate surfaces.

However, the chemical functionalization of organic solids and carbon materials, in particular, is a complex process as the substrates are insoluble; therefore, the reaction must be conducted either in bulk or in a heterogeneous medium. Because of the heterogeneous nature of the reactions, the modification reactions are often incomplete and will form multiple products with variable degrees of functionalization. More importantly, carbon materials, such as carbon black, graphite, graphene, and CNTs, are not monodisperse, particularly in diameter and length. A small difference in the degree of functionalization with organic compounds will introduce solubility variations in the functionalized products during the reaction. As a result, the availability of the carbon nanomaterials that are partially solvated for further reaction will increase, and the reaction will proceed discriminately with respect to the size and the degree of functionalization. Thus, it is difficult to control the efficiency and the specificity of organic reactions with carbon materials, especially with respect to the placement of functional groups and the degree of

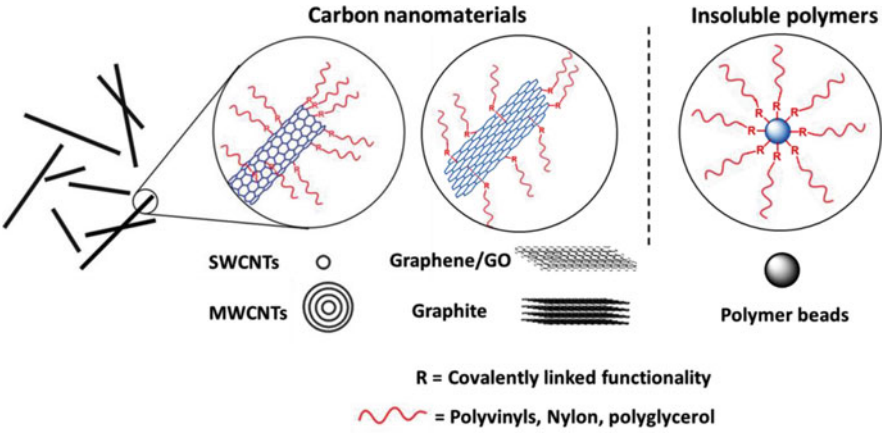

Scheme 4 Organic substrates containing sp^2 carbon back-bone nanomaterials used in surface-initiated anionic polymerization

functionalization on a molecular basis. Nevertheless, the attachment of organic moieties on the sp^2 graphitic carbons introduces an organophilic character and helps dispersing carbon nanomaterials in bulk polymers and in organic solvents. Although the modification affects some inherent properties of carbon nanomaterials, it significantly increases their potential applications.

3.1 Anionic Polymerization from Graphitic Carbon Nanomaterials

In early 1960s, researchers from Japan reported anionic polymerization of styrene from the surface of carbon black-alkali metal complex [67]. This initial result prompted exploration of the possibility to grow polymer chains from the surface of various carbon materials using anionic polymerization for the development of enhanced polymer composites. Ohkita and coworkers [68] attempted the polymerization of styrene from carbon black catalyzed by *n*-BuLi via grafting-from and grafting-to methods. They found a marked retardation of the polymerization, likely due to the preferential reaction between *n*-BuLi and the oxygen-containing groups on the carbon black. Tsubokawa et al. demonstrated anionic grafting of poly(*β*-propiolactone) from carbon black initiated by the surface carboxylate groups [69] and the anionic grafting of PMMA or PS from carbon whisker using *n*-BuLi/TMEDA complexes as metalating agent (Scheme 5) (Table 1, entry 10) [34].

Graphite is another important substrate that has drawn considerable attention recently [70, 71]. Studies concerning graphite functionalization are occasionally presented in the literature since the early 1960s [72]. Most of the reports describe grafting vinyl polymers from graphite-alkali metal intercalation compounds [73]. Sun and coworkers reported initiation of styrene from the surface and the edges of the K-intercalated graphite [74]. Although this and other publications never caught much attention, the emergence of the graphene research in recent years has attracted significant interest in SIAP. A majority of the publications in this area deals with grafting polymers from surfaces using ATRP, due to its simplicity among other modern controlled radical polymerization processes [75–79]. Nevertheless, anionic polymerization has been used in some cases to take advantages of its process controls (Table 1).

Tour and coworkers reported SIP of styrene via anionic polymerization using anions generated from unzipping of MWNTs in the presence of potassium metal [35]. They claimed that the carbanions are generated via reduction of edge radicals

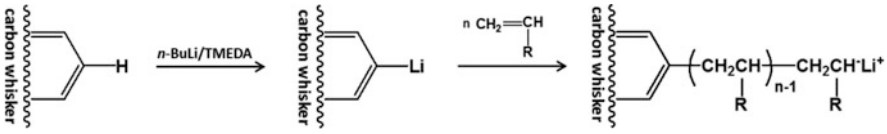

Scheme 5 Anionic polymerization of vinyl monomers from carbon whisker

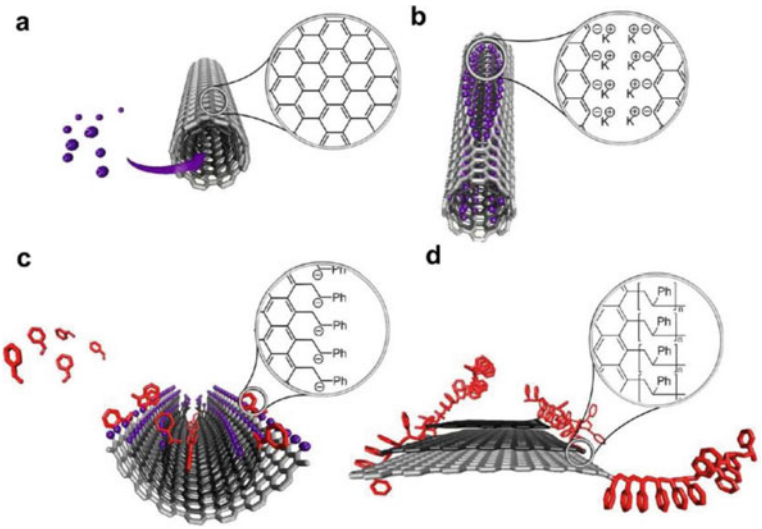

Fig. 9 Reaction scheme for the one-pot synthesis of functionalized GNRs. (**a**) The MWNTs are intercalated with potassium naphthalenide (*blue dots*). (**b**) A longitudinal fissure is formed in the walls of the MWNTs. (**c**) Polymerization of styrene (for instance) assists in exfoliation of MWNTs. (**d**) PF-GNRs are formed upon quenching (Reproduced with permission from Ref. [35], Copyright 2013 ACS)

during the reaction and can be used for the anionic polymerization. As the anions are believed to be generated during unzipping, they are selectively located at the edges of graphene nanoribbons (GNR) (Fig. 9). However, the amount of PS grafted-from such as nanoribbons was reported to be low (~9 wt %, for THF reaction), which may indicate that the formation of anions on the GNR is insufficient for the initiation, or the propagating anions undergo termination, or the sequential reduction of anion radicals is not prevalently occurring. Any of these factors may be responsible for a low graft-density observed by the authors (Table 1, entry 11). It should be mentioned here that the grafting of PS, $M_n = 5{,}000$ g/mol, for example, on every edge carbon for a theoretical rectangular GNR of 1,000 nm^2 at its length sides would exceed 99 wt % PS. Thus, the grafting efficiency is far less than the reaction scheme proposed in Fig. 9. Although unzipping is clearly evident by TEM images, the dispersion of GNR in any medium without appropriate functionalization would be difficult.

In another study, Zhang et al. used graphene oxide (GO) as a substrate for grafting polymers [36]. By taking advantage of readily accessible oxygen-containing groups on GO, the functional groups are reacted with isocyanate and then used for grafting nylon 6 via anionic ring-opening polymerization (ROP) of ε-caprolactam (Scheme 6, Fig. 10). The authors carefully studied the formation of key intermediates using nuclear magnetic resonance (NMR), FTIR, and XPS

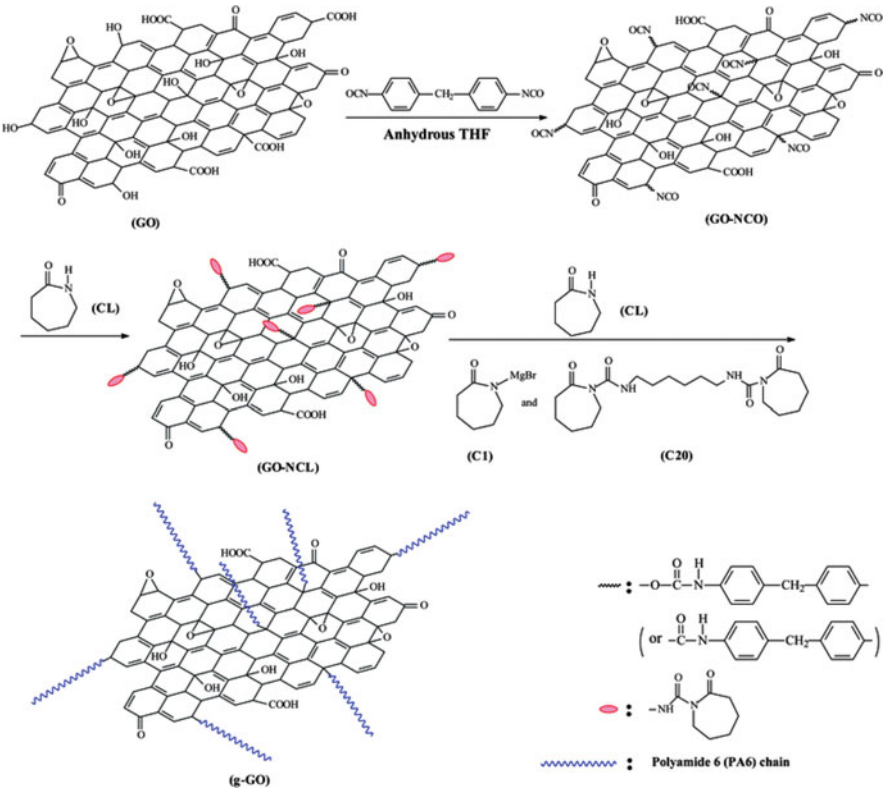

Scheme 6 Synthetic scheme of the modification of graphene oxide (GO) with caprolactam and subsequent grafting of nylon 6 by in situ anionic ring-opening polymerization (Reproduced with permission from Ref. [36], Copyright 2012 RSC)

spectroscopies and provided structural information about the nylon-grafted GO (Table 1, entry 12). The modification of GO was shown to enhance the mechanical and thermal properties of the corresponding nylon composites.

3.2 Anionic Polymerization from Carbon Nanotubes

The living nature of anionic polymerization [80] with its ability to afford polymers of narrow MWD and high molecular weight in a controlled way, even at very low initiator concentration, has made it an attractive choice in grafting polymers from CNTs. Viswanathan et al. [37] were the first to grow polymer from nanotubes via anionic polymerization. They introduced carbanions on the surface of the SWNTs through addition of *sec*-BuLi to the sp^2 carbons. The resulting resonance-stabilized carbanion on the SWNTs was used as initiating site for the polymerization of styrene. It was stated that a mutual electrostatic repulsion between the individual nanotubes could exfoliate the SWNT bundles. The amount of carbanion generated

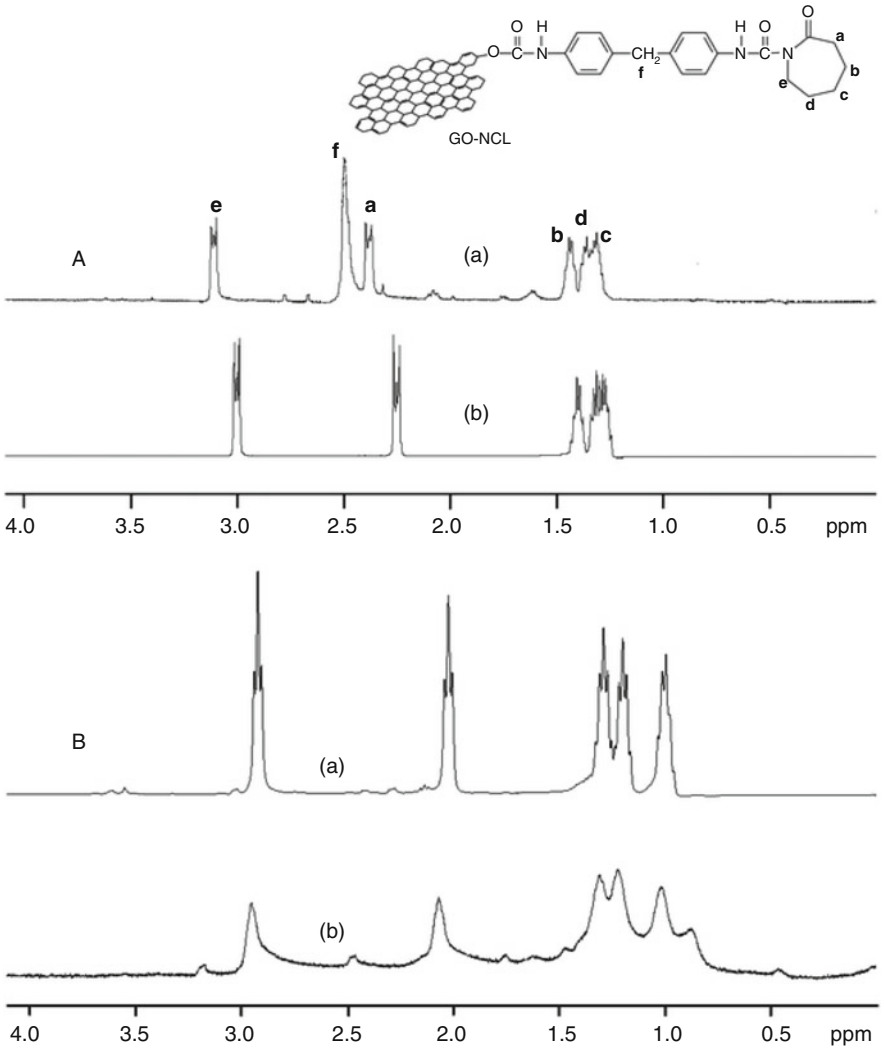

Fig 10 (**a**) ^{1}H NMR spectra of functionalized GO (*a*) and ε-caprolactam (*b*) in deuterated formic acid solution. (**b**) ^{1}H NMR spectra of nylon 6 (*a*) and *g*-GO (*b*) in deuterated formic acid solution (Reproduced with permission from Ref. [36], Copyright 2012 RSC)

on the SWNTs was not determined as the styrene polymerization was conducted in situ in the presence of free *sec*-BuLi. Thus, a concurrent solution polymerization produced PS nanocomposite consisting of MWNTs-*g*-PS. Grafting efficiency was determined after removing the free PS from MWNTs-*g*-PS through a solvent wash by TGA, and it was found to be very low (~10–15 wt %) (Table 1, entry 13). The functionalization with butyl groups and grafted PS was confirmed via Raman spectroscopy, which showed some differences in D/G ratio of the peaks (Fig. 11).

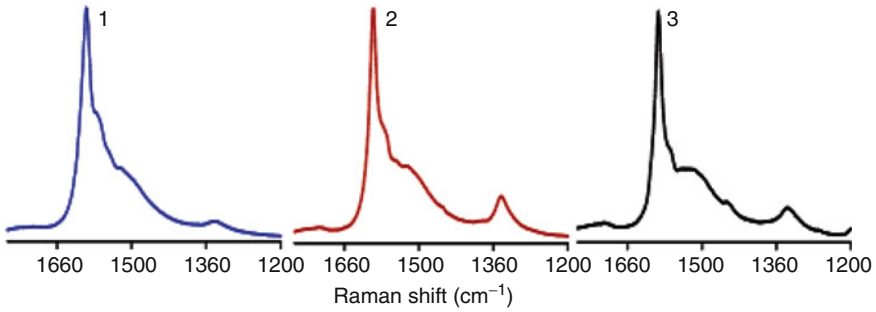

Fig. 11 Raman scattering spectra (514.4 nm) of (*1*) pristine SWNTs, (*2*) butylated SWNTs, and (*3*) PS-grafted SWNTs (Reproduced with permission from Ref. [37], Copyright 2003 ACS)

The observed T_g of the grafted PS in MWNTs-*g*-PS was higher by 15 °C than PS. More importantly, the PS-grafted SWNTs rendered excellent composites that had higher thermal stability even with very low nanotube loading (0.05 wt %), exhibiting good filler dispersion in the polymer matrix.

Using the same approach, Chen et al. [38] showed that the carbanions on the surface of SWNTs can initiate the polymerization of *tert*-butyl acrylate (*t*-BA) but not that of methyl methacrylate (MMA) (Scheme 7). The authors suggested that a possible reason for this behavior was the difference in the reactivity of the two monomers toward the delocalized carbanions on the SWNTs. However, the actual reason for this behavior is not clearly understood as the reactivity of the generated carbanions on the SWNTs was sufficient enough to initiate styrene as shown by Ajayan et al. [37]. Thus, the reactivity differences of the monomers may not be the reason for their observation. Nevertheless, the living nature of the polymerization was confirmed by initiating MMA from the growing P*t*BA enolate anions. The same group also synthesized a diblock copolymer (P*t*BA-*b*-PMMA) from SWNTs with 47 wt % polymer (Scheme 7, Table 1, entry 14).

On the other hand, Liang et al. [39] reduced SWNTs in the presence of Li in ammonia as anionic initiators for the polymerization of MMA.

They showed that an addition of Li/NH_3 to SWNTs leads to SWNT salts that have the ability to exfoliate SWNT bundles and grow PMMA. The CNTs with 45 wt % polymer were synthesized, and the average thickness of an amorphous polymer layer around the SWNTs was 1.0–1.5 nm, as calculated by AFM (Table 1, entry 15). The authors observed a noticeable Raman D-band in the "PMMA-grafted SWNTs" (Fig. 12). However, based on this single piece of evidence alone without a side-by-side comparison with control experiment, they concluded covalent linkage between PMMA chains, and the CNT surface. The enhanced D-band could arise simply from a Birch-like reduction of the preexisting defects in the nanotubes. The radical anion on the SWNTs and the presence of solvated electrons in Li/NH_3 solution can contribute for the formation of PMMA, and hence an inefficient washing of the SWNTs after the reaction may also produce similar results.

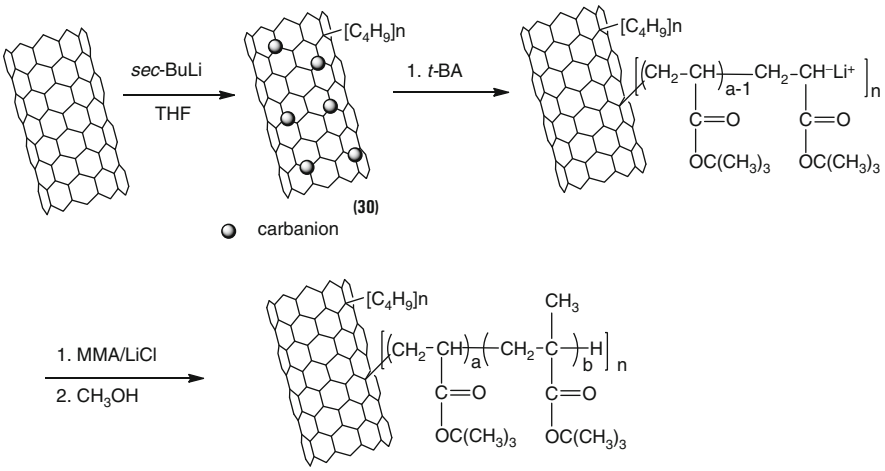

Scheme 7 Anionic polymerizations of methyl acrylate and methyl methacrylate from SWNTs and SWNT-*g*-(P*t*BA), respectively (Reproduced with permission from Ref. [77], Copyright 2013 RSC)

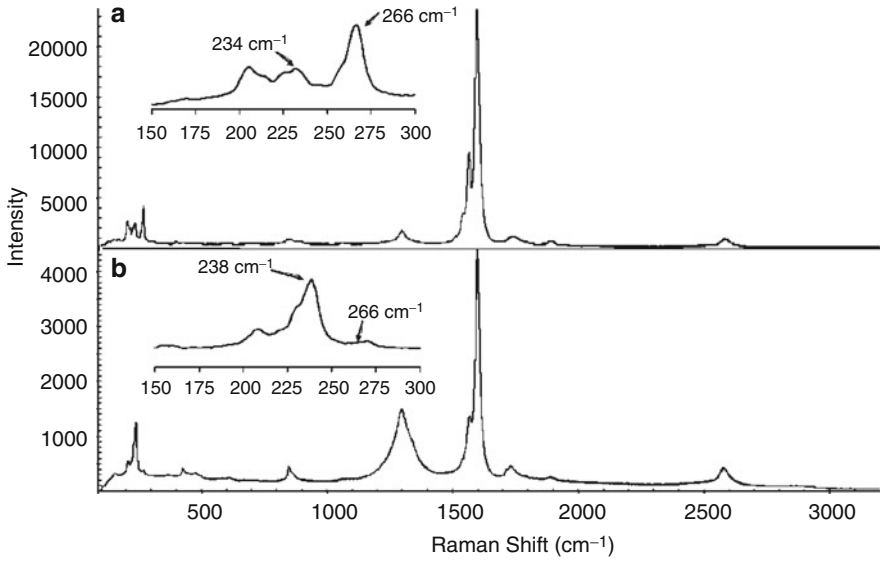

Fig. 12 Raman spectra (780 nm excitation) of pristine SWNTs (**a**) and PMMA-grafted SWNTs (**b**) (Reproduced with permission from Ref. [39], Copyright 2006 ACS)

In order to achieve a higher grafting efficiency with high molecular weight polymers, Baskaran and coworkers used a different approach [40] to grow PS from MWNTs via anionic polymerization. As mentioned previously, the direct reaction of *sec*-BuLi with the sp^2 carbon of MWNTs was inefficient [81, 37].

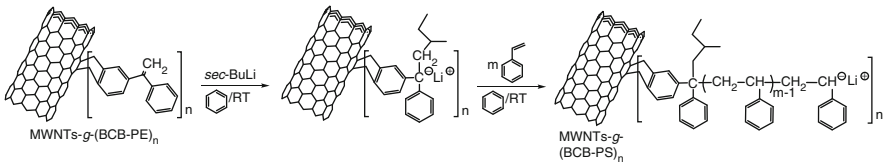

Scheme 8 Anionic polymerization of styrene from MWNTs-*g*-(BCB-PE)-grafted tubes in benzene at RT (Reproduced with permission from Ref. [40], Copyright 2008 ACS)

Therefore, they generated carbanion sites away from the CNT surface. Accordingly, the MWNTs were covalently functionalized with 1-benzocylcobutene-1-′-phenylethylene (BCB-PE) through a [4 + 2] Diels-Alder cycloaddition [82]. A statistical distribution of covalent attachment of the substituted diphenylethylene, a precursor initiator, was introduced throughout the surface of MWNTs. The presence of the olefin was confirmed by FTIR, Raman spectroscopy, and TGA. Reactive carbanions were generated from MWNTs-*g*-(BCB-PE)$_n$, by addition of *sec*-BuLi. The polymerization of styrene was initiated in benzene at room temperature under high-vacuum condition (Scheme 8). Although the typical red color of the phenylhexyllithium anion on the MWNTs was not seen, probably due to an intense black color of the solution, resulting from the gradual dispersion of PS-grafted MWNTs, the initiation of styrene from the surface-grafted phenylhexyllithium anions was found to be slow. This was attributed to the heterogeneous nature of the reaction. A small amount of MWNTs-*g*-initiator was insoluble in the reactor during the polymerization for about an hour. On the other hand, the polymerizations carried out for more than 90 min showed a complete dispersion of MWNTs during the polymerization. The surface-grown polymers were obtained in high conversion, forming MWNTs-*g*-PS containing only a small fraction of MWNTs (<1 wt %). A control polymerization of styrene was carried out using *sec*-BuLi in the presence of pristine MWNTs. Upon addition of styrene, an orange color appeared immediately indicating the initiation of styrene from the free initiator present in the solution. After the termination of the polymerization, the MWNTs were recovered by a thorough solvent wash in THF to remove the free PS. The recovered MWNTs did not have grafted PS as confirmed by TGA and transmission electron microscopy (TEM) analysis in the control experiment.

The MWNTs-*g*-PS were characterized by FTIR, ^{1}H-NMR, Raman spectroscopy, differential scanning calorimetry (DSC), TGA, and TEM. The TEM images showed the presence of a thick layer of polymer (~30 nm) around the surface of MWNTs (Fig. 13, Table 1, entry 16). The formation of diblock copolymer, MWNTs-*g*-PS-*b*-PI, confirmed the living nature of the polymerization from the surface.

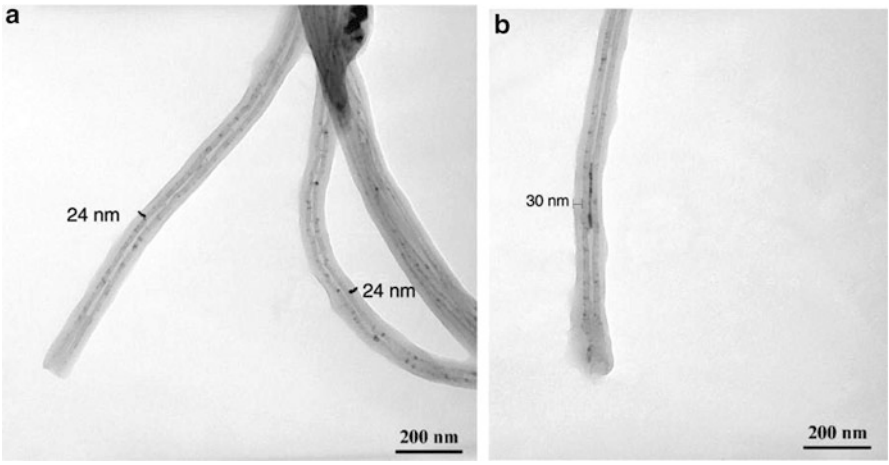

Fig. 13 TEM images of surface-grown PS exhibiting 24 nm (**a**) and 30 nm (**b**) PS layer on the surface of MWNTs (Reproduced with permission from Ref. [40], Copyright 2008 ACS)

3.3 Anionic Ring-Opening Polymerizations from Carbon Nanotubes

Aliphatic polyesters, such as poly(*p*-dioxanone), poly(*ε*-caprolactone), poly(L-lactide), polyethers (e.g., PEO), and polypeptides, are biocompatible and in most cases biodegradable polymers. These materials have been proven to be useful as scaffold in implantable medical devices, as surgical sutures and in drug delivery systems, since they eliminate the need for removal of the device after being used. Their synthesis involves ROP techniques [83]. Grafting polyether, polyamide, and polyester from CNTs is very important as these materials can be used as fillers in developing nanocomposites in commodity plastics to enhance mechanical property. The ROP can be performed by several initiating systems such as anionic, cationic, coordination, and metathesis.

3.3.1 Polyesters

Yoon et al. [41] used ROP to graft poly(*p*-dioxanone) (PPDX) from SWNTs via the grafting-from method. The surface of SWNTs was covalently attached with 6-amino-1-hexanol by reacting with the acid chloride-functionalized SWNTs in dimethylformamide (DMF). The produced hydroxy-functionalized SWNTs-$(OH)_n$ were then used for the initiation of *p*-dioxanone, in the presence of tin(II) 2--ethylhexanoate ($Sn(Oct)_2$). They found that the thermal stability of the grafted PPDX increased after the covalent attachment onto the SWNTs. The SWNTs-*g*-PPDX had no noticeable transition corresponding to T_g and T_m up to 125 °C,

although the pure PPDX showed these transitions at −13.4 and 103 °C, respectively. The changes in the grafted PPDX properties were attributed to a strong interaction between SWNTs and PPDX and a decreased mobility of the PPDX chains.

Several methods have been reported to introduce hydroxyl groups on CNTs for the polymerization of ε-caprolactone and other monomers using ROP [84–86]. The reaction of pristine MWNTs with various azide compounds via 1,3-cycloaddition [84], the use of diradicals via Bergman cyclization [85], and the conversion of acid groups of MWNTs to azide for copper-catalyzed Huisgen's 1,3-dipolar cycloaddition [86] with various functional alkynes are a few of these methods.

Buffa et al. [44] functionalized SWNTs produced by the CoMoCAT process, with 4-hydroxymethylaniline (HMA) via the diazonium salt method. The SWNTs-$(OH)_n$, generated by the functionalization, were then used to polymerize ε-caprolactone, in the presence of stannous octanoate as a catalyst. The dispersion of SWNTs grafted with poly(ε-caprolactone) (PCL) was tested in chloroform. A dramatic increase compared to that of neat SWNTs was observed due to the high solubility of PCL in chloroform. TGA of the samples indicated that the amount of PCL grafted was 63 wt % (Table 1, entry 20), while a combined TPD (temperature-programmed desorption)/TPO (temperature-programmed oxidation) technique revealed that the average polymer length was only 5 monomeric units. According to the authors, the two main factors for the limited growth of the grafted chains were the presence of nanotubes in the polymerization medium and the presence of adsorbed water on the CNT surface. The former acts as terminators while the latter as initiator generating a large amount of "free" PCL. Accordingly, it was suggested that an increase in the length of the PCL attached to the nanotubes can only be achieved when the adsorbed water from the nanotubes is eliminated.

In a similar work [45], the hydroxyl groups were introduced on the MWNT surfaces by reacting oxidized MWNTs with excess thionyl chloride and then with glycol. The -OH-functionalized MWNTs were used for the surface-initiated ROP of ε-caprolactone, in butanol at 120 °C in the presence of stannous octanoate. The content of the grafted polymer and the molecular weight of the free polymer initiated by the butanol were increased with increasing the feed ratio of monomer to initiating sites. The polydispersity indices of the free polymer were very broad reaching even 13.0, which was ascribed to the increased possibility of chain termination due to the presence of the CNTs. However, the actual mechanism of the propagating PCL anion undergoing termination with the sp^2 carbon network was not discussed. Biodegradation of the recovered MWNT-*g*-PCL was tested by using pseudomonas lipase as a bioactive enzyme catalyst. It was revealed that the grafted PCL chains retained their biodegradability and were completely degraded within 4 days.

The influence of MWNT-*g*-PCL on vapor sensing properties was investigated, by Castro et al. [46], for a series of conductive polymer composite (CPC) transducers. MWNTs-*g*-PCL were prepared by first reacting MWNTs-$(OH)_n$ with trimethylaluminum (catalyst) to produce aluminum alkoxide initiator followed by the anionic coordination ROP of ε-caprolactone (Scheme 9). AFM observations

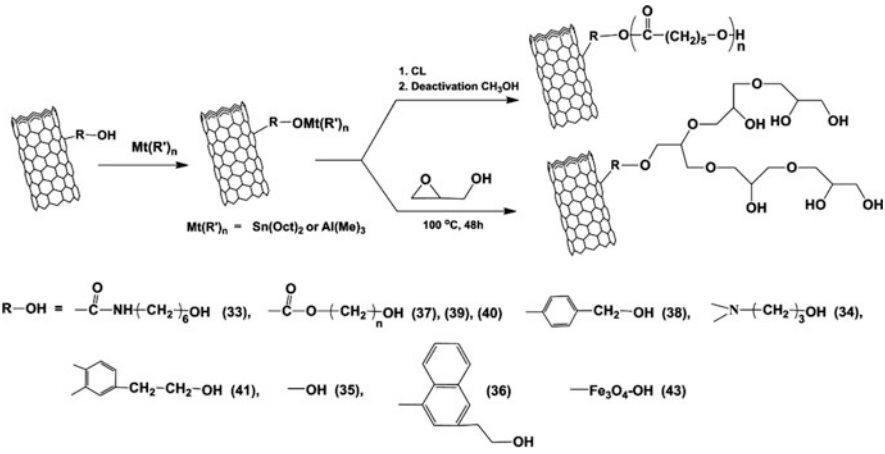

Scheme 9 Synthesis of MWNT-g-PCL and MWNTs-g-HPG using different types of initiators via anionic coordinative ring-opening polymerization (Reproduced with permission from Ref. [77], Copyright 2013 RSC)

allowed an evaluation of the MWNT coating and dispersion levels. Sensors were prepared by spray coating layer-by-layer MWNT-*g*-PCL solutions onto the interdigitated copper electrodes that had been etched by photolithography onto an epoxy substrate. Chemo-electrical properties of CPC sensors exposed to different vapors (water, methanol, toluene, tetrahydrofuran, and chloroform) were analyzed in terms of signal sensitivity, selectivity, reproducibility, and stability. The MWNT-*g*-PCL sensors displayed a very good discrimination capability for all the vapors above (polar and nonpolar), which allowed for the preparation of sensors with a large detection spectrum. The chemo-electrical properties of the sensors exposed to different vapors were found to be reproducible, and the electrical signals displayed reversibility with a fast recovery.

A different synthetic approach for the grafting of ε-caprolactone on MWNTs was presented by Ruelle et al. [47]. MWNTs were placed under an atomic nitrogen flow formed by the dissociation of molecular nitrogen in $Ar + N_2$ mixed microwave plasma in order to covalently functionalize with primary and secondary amines. The amino-MWNTs were activated by triethylaluminum and then used as an initiator for ROP of ε-caprolactone. As revealed by TEM, functionalization was inhomogeneous, and the MWNTs had a high (10 atomic % N) of amine functionalization on the plasma exposed surface of the sample.

Biodegradable supramolecular hybrids of MWNT-*g*-PCL and α-cyclodextrins (α-CDs) (inclusion complexes), with potential applications in medicine and biology, were prepared by Yang et al. [48]. First, MWNTs were functionalized with hydroxyl groups (MWNTs-$(OH)_n$) via a nitrene cycloaddition with appropriate reagent. The reaction was followed by the surface-initiated ROP of ε-caprolactone in the presence of a metal catalyst to afford MWNTs-*g*-PCL. The TGA showed about 58 wt % of PCL was grafted onto the MWNTs and TEM images revealed the

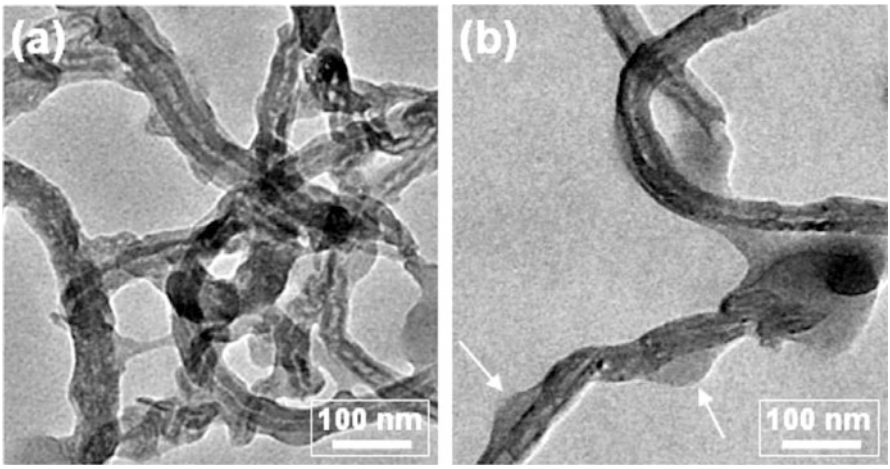

Fig. 14 TEM images of MWNTs-*g*-PCL complexed with α-CDs (**a** and **b**) (Reproduced with permission from Ref. [48], Copyright 2010 Elsevier)

presence of polymer layers with thicknesses in the range of 5–7 nm on the surface of the MWNTs (Table 1, entry 24). Inclusion complexes were formed by hydrogen bonds between the hydroxyl groups of α-CDs and the carbonyl groups of PCL, indicating that supramolecular polypseudorotaxanes were formed through α-CD channel threading onto the PCL chains of MWNT-*g*-PCL (Fig. 14). However, the size of uneven pimples shown in Fig. 14 was very large that it couldn't be interpreted only for supramolecular polypseudorotaxane formation. It is important to mention that the α-CD is also known to get adsorbed onto the CNTs [87]. Therefore, the contribution of adsorption and its influence on the reported results are not known.

Poly($_L$-lactide) (PLLA) is widely used in tissue engineering, drug delivery systems, and implant materials due to its excellent biocompatibility and biodegradability. However, the mechanical properties of PLLA for high load-bearing biomedical applications are insufficient. The PLLA nanocomposite containing CNTs has been implied to enhance the mechanical properties for various applications. The first attempt to polymerize $_L$-LA from the surface of MWNTs was reported by Chen et al. [51]. Carboxylic acid-functionalized MWNTs were treated with $SOCl_2$, and the acyl chloride-containing CNTs were further reacted with butanediol in order to introduce hydroxyl groups on the surface. The polymerization of $_L$-LA was performed in the presence of stannous octanote. The amount of grafted PLLA increased with time depending on the polarity of the reaction medium. When the polymerization was carried out in DMF, the amount of grafted PLLA on the MWNTs was higher than that obtained in toluene.

Nanocomposites of PLLA with MWNTs-*g*-PLLA were prepared and tested for mechanical property enhancement. The authors claimed that the incorporation of 1 wt % of MWNT-*g*-PLLA in PLLA matrix didn't show any indication of

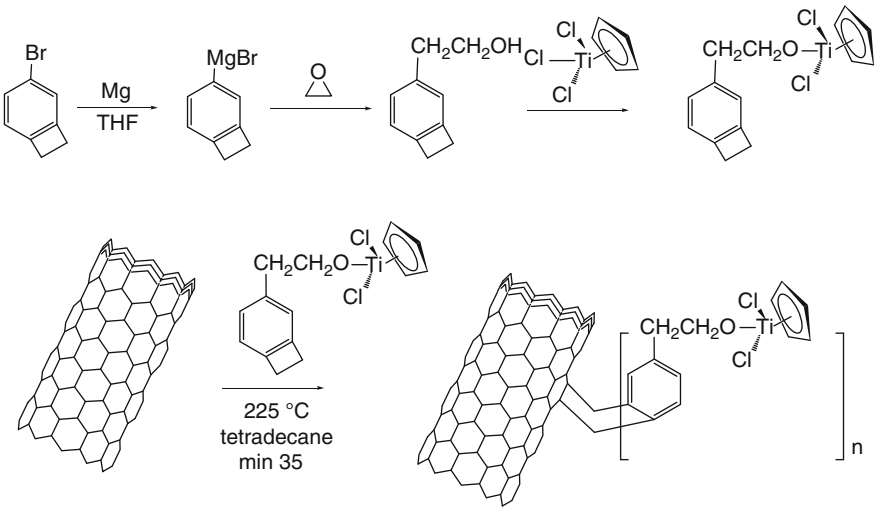

Scheme 10 Grignard synthesis of (1-benzocyclobutene ethoxy) dichlorocyclopentadienyl-titanium (BCB-EOTiCpCl$_2$) and covalent functionalization of MWNTs using a [4 + 2] Diels-Alder cycloaddition reaction (Reproduced with permission from Ref. [54], Copyright 2009 ACS)

aggregation based on SEM, and the nanocomposites exhibited high tensile strength and modulus rendering PLLA more resistant to deformation. Thermal stability, electrical conductivity, as well as mechanical properties of PLLA nanocomposites containing MWNT-*g*-PLLA were also studied [53, 52]. Good interfacial adhesion between MWNTs and the polymer matrix in PLLA/MWNT-*g*-PLLA composites also increased the activation energy compared to PLLA/MWNT, indicating that the former was thermally more stable.

Recently, Priftis and coworkers [54] used a titanium alkoxide catalyst (TiCpCl$_2$) to polymerize $_L$-LA, ε-CL, and *n*-hexyl isocyanate from SWNTs and MWNTs. A Diels-Alder cycloaddition was used to covalently attach benzocyclobutene functionalized with titanium alkoxide, to the sidewalls of CNTs (Scheme 10). The grafted CNTs were used for the titanium-mediated SIP of different monomers. Kinetic study of the $_L$-LA polymerization indicated that the initiation was very slow and characterized by an induction period of about 4 h. After this period, the polymerization medium became homogeneous; the polymerization proceeded fast giving enhanced efficiency for grafting polymers on the CNTs, and the viscosity of the reaction medium was substantially increased in less than 5 h. The long induction period could be attributed to a steric hindrance of MWNT-titanium complex for the initiation. Titanium-mediated coordination polymerization of $_L$-LA, using the same solvent and catalyst, in the absence of CNTs had also an induction period of an hour. The grafted polymer content could be adjusted using the reaction time, when the mole feed ratio of monomer to the grafted initiator was kept constant. A control experiment was performed in which a known amount of the precursor catalyst CpTiCl$_2$(OCH$_2$CH$_3$) was mixed with pristine CNTs in order to study the influence

of Cp ring adsorption onto the CNTs through π-π stacking. A similar procedure as for the MWNTs-*g*-BCB-EOTiCpCl$_2$ was used for the polymerization and found that the MWNTs could be recovered after the polymerization without any polymer grafted on it. This confirmed the absence of polymer adsorption. The polymerization of ε-CL showed a similar trend as the L-LA, while in the case of *n*-hexyl isocyanate the monomer conversion was very low (10 %) even after 20 h of the polymerization.

Cai and coworkers [55] used MWNT-(OH)$_n$ for the copolymerization of L-lactide and ε-caprolactone in the presence of stannous octanoate as the catalyst. The copolymer poly(L-lactide-*co*-caprolactone) nanocomposites with MWNT-*g*-poly(L-lactide-*co*-caprolactone) showed an increase in tensile strength and a decrease in elastic modulus compared to the neat copolymer. The same group used MWNTs that were first functionalized with FeO_4-OH for the polymerization of L-LA. The PLLA nanocomposite materials prepared with MWNTs-*g*-PLLA exhibited superparamagnetic performance, and it was possible to align under low magnetic field [56].

3.3.2 Polyethers

Grafting polyethylene oxide (PEO) from CNTs will enable dissolution of CNTs in water and can be used for medical applications. Baskaran and coworkers polymerized ethylene oxide (EO) via anionic ROP from MWNTs functionalized with hydroxyl groups (Scheme 11) [40]. The MWNTs were first covalently functionalized with 4-hydroxyethyl benzocyclobutene (BCB-EO) through [4 + 2] Diels-Alder cycloaddition. The attachment of the BCB-EO, a hydroxyl precursor, was confirmed by FTIR, Raman spectroscopy, and TGA. Polymerization of ethylene oxide was performed under high vacuum using break-seal technique (Fig. 15a). Triphenylmethyl potassium was used to convert the hydroxyl groups on the surface of MWNTs into alkoxide anions. As alkoxide anions exist in rapid equilibrium with the remaining hydroxyl groups in the presence of potassium counterion, a minimum of 30 mol %, hydroxyls was converted into alkoxide anions. The initiation of ethylene oxide from the surface alkoxy anions was very slow. The heterogeneous nature of the reaction and the aggregation of alkoxide anions in the presence of MWNTs could be attributed to a slow propagation. However, at a constant mole

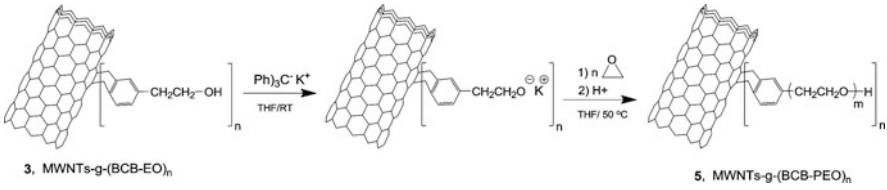

Scheme 11 Surface-initiated anionic polymerization of ethylene oxide from MWNTs-*g*-(BCB-EO)$_n$ surface (Reproduced with permission from Ref. [40], Copyright 2008 ACS)

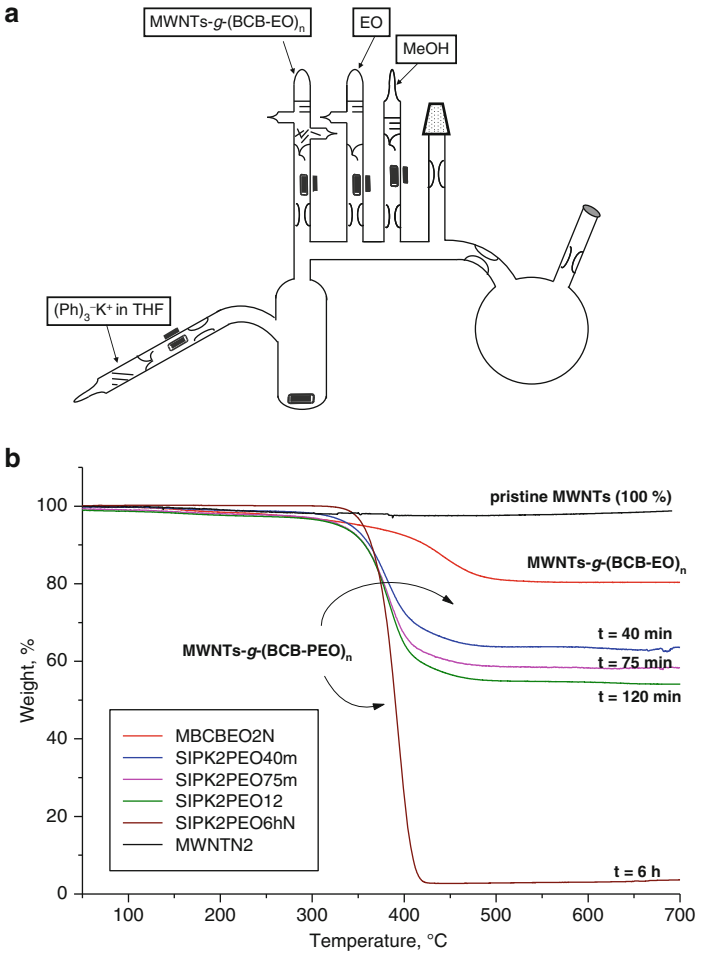

Fig. 15 (**a**) All-glass reactor used for the surface-initiated anionic polymerization of ethylene oxide from MWNTs and (**b**) TGA of MWNTs-*g*-(BCB-PEO)$_n$ at various reaction times in the surface-initiated anionic polymerization of ethylene oxide from MWNTs-*g*-(BCB-EO)$_n$ in THF at 40 °C (Reproduced with permission from Ref. [40], Copyright 2008 ACS)

ratio of monomer to the grafted initiator, the amount of grafted polyethylene oxide (PEO) increased gradually with increasing the polymerization time. The monomer conversion also increased gradually with polymerization time reaching a maximum of 57 % after 48 h, indicating a slow propagation of the surface polymerization (Fig. 15b). The surface-grown polymers were obtained in high wt fraction, forming MWNTs-*g*-PEO containing only a small fraction of MWNTs <4 wt % (Table 1, entry 16).

For samples obtained after a long polymerization time, it was not possible to filter the reaction solution through a Teflon membrane, and the samples were

recovered by precipitation in non-solvent. Size exclusion chromatography (SEC) analysis, using light scattering detector, of these samples showed the presence of multiple peaks. This was attributed to the fact that MWNTs are broadly distributed in terms of length, diameter, and also chemical functionality. Although these samples could be analyzed using SEC, with a styrene-divinylbenzene cross-linked gel column, an efficient resolution of different molecules based on their size is not possible. The hydrodynamic volume of MWNTs-*g*-PEO is expected to be very high as the tubes are long, and most of them will pass through interparticle gaps rather than getting into the pores. Therefore, such an analysis would only give an apparent molecular weight that can be used for a relative comparison within a set of experiments. One must be careful in treating the $M_{n,(app)}$ obtained from SEC due to the reasons mentioned above. Nevertheless, the MWNT-*g*-PEO samples taken at different polymerization time showed (in SEC) an increase in apparent molecular weight indicating overall control on the molecular weight of the grafts is possible in these reactions. Light scattering detector showed multiple peaks corresponding to a few thousands to few millions in weight average molecular weight, confirming the presence of multiple distributions of high molecular weight species. The TEM images showed the presence of thick layers of grafted PEO, nonuniformly distributed along the whole surface (Fig. 16).

Very recently, Sakellariou et al. [49] studied the kinetics of ROP of ε-CL from MWNTs and the crystallization behavior of the MWNTs-g-PCL together with that of MWNTs-*g*-PEO. The polymerization could be controlled with time, though the reaction proceeded rapidly. As revealed by TGA, a 98 wt % PCL was grafted after 4 h, and 70 % monomer conversion was achieved (Table 1, entry 25). A remarkable

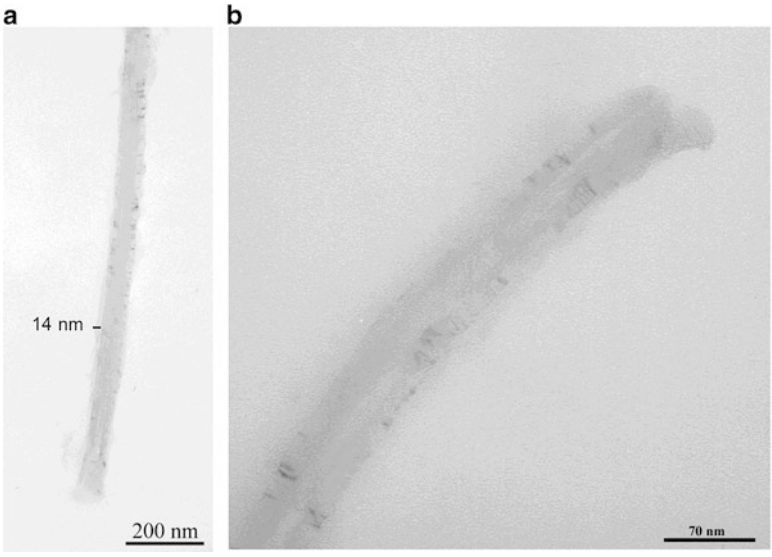

Fig. 16 TEM images of MWNTs-*g*-(BCB-PEO)$_n$ (**a**, **b**) with nonuniform PEO-grafted chain on the surface of MWNTs (Reproduced with permission from Ref. [40], Copyright 2008 ACS)

nucleation effect was observed by the incorporation of MWNTs that reduced the supercooling needed for crystallization of both PCL and PEO. Furthermore, the isothermal crystallization kinetics of the grafted PCL and PEO were substantially accelerated compared to the neat polymers, which were attributed to the anchoring of the chain ends to the MWNTs via covalent bonding.

In another study by Sakellariou et al. [50], diblock copolymers were grafted onto MWNTs via a combination of polymerization techniques. Using the same method above, a substituted benzocyclobutene containing hydroxyl group was attached on the surface of MWNTs and later used for the polymerization of EO or ε-CL. The hydroxyl groups of the grafted polymer chain ends were used for the initiation of second block. Accordingly, the chain ends of the MWNTs-*g*-PEO were used as ROP macroinitiator for the polymerization of ε-CL resulting in biocompatible MWNT-*g*-(PEO-*b*-PCL). By esterification of the hydroxyl PEO end groups with excess 2-bromoisobutyryl bromide, an ATRP macroinitiator was obtained and used for the polymerization of styrene and 2-(dimethylamino)ethylmethacrylate (DMAEMA) resulting in diblock copolymer grafted MWNTs, which had very high (>90 wt %) grafted polymer content (Table 1, entry 25). This strategy, through a combination of two different polymerization techniques, widens the opportunities for the synthesis of even more complex macromolecular structures on the CNT surface.

Gao's group [42] performed anionic ROP of glycidol (2,3-epoxy-1-propanol) in dioxane using potassium methoxide as a catalyst, to grow hyperbranched polyglycerol (HPG) from MWNT-$(OH)_n$ surfaces. The macroinitiator, MWNT-OH, was prepared by reacting with 2-azidoethanol in N-methyl-2-pyrrolidone. The amount of grafted HPG was adjusted, up to 90 wt %, by changing the feed ratio of glycidol to MWNTs-$(OH)_n$ (Table 1, entry 18). When the polymerization was conducted in bulk, the grafted polymer content was never higher than 45 wt %, even at high feed ratios of glycidol to MWNTs-$(OH)_n$. The authors ascribed this phenomenon to the higher viscosity of the reaction mixture in the bulk polymerization. In fact, an extended aggregation of propagating center with potassium counterion and a lack of solvation of counterion could be the other reasons for poor conversion of HPG in the absence of solvent. A concurrent self-condensing ROP of glycidol through counterion exchange to the monomer was monitored. The number average molecular weights of the free HPGs increased linearly with increasing feed ratio of monomer to initiating site, and the polydispersity indices were relatively low (<1.8). Although the authors claimed that the polymerization had a living character, such a high MWD confirms that the polymerization proceeded with severe side reactions in the presence of CNTs. The HPG grafted MWNTs (MWNTs-*g*-HPG) were recovered by dispersion in methanol, followed by centrifugation and washing several times with excess methanol. The remaining solid, MWNTs-*g*-HPG, was dried overnight. By reacting to the hydroxy groups of the grafted HPG with palmitoyl chloride, they produced MWNT-*g*-amphiphilic hyperbranched polymers. The resulting product showed good solubility in weak polar or nonpolar solvents in contrast to MWNTs-*g*-HPG, which were soluble only in strong polar solvents. Fluorescent MWNTs were also prepared by attaching rhodamine 6B molecules to the surface of MWNT-*g*-(HPG). The abundance of

functional groups on the surface of CNT hybrids can be used as a nanoplatform to conjugate functional molecules for further application in drug delivery, cell imaging, and bioprobing.

Another route for the synthesis of biocompatible and biodegradable CNT hybrids was reported by Adeli et al. [43]. Hyperbranched molecular trees were grown from the surface of MWNTs via in situ anionic ROP of glycidol as described in Scheme 9. Short-term in vitro cytotoxicity and hemocompatibility tests were conducted on HT 1,080 cell line (human fibrosarcoma) for MWNTs-*g*-HPG. The results showed no sign of toxicity for concentrations up to 1 mg/mL after 24 h of the incubation.

3.3.3 Poly(peptides) and Polyamides

Primary amine acts as an initiator for the polymerization of cyclic amino acids via N-carboxyanhydride (NCA) method to produce polypeptides with controlled molecular weight [88]. The ROP was used to graft a polypeptide from the surface of MWNTs [57]. Oxidized MWNTs were converted into an amine-functionalized MWNTs by amidation of the carboxylic groups with excess of 1,6-diaminohexane. The MWNTs-$(NH_2)_n$ were then used for ROP of γ-benzyl-*L*-glutamate N-carboxyanhydride (BLG-NCA) (Scheme 12). The resulting hybrid material exhibited core-shell morphology with thickness of the polypeptide layer ranging from 4 to 22 nm. The thickness of the polypeptide could not be controlled by the feed ratio of NCA monomer to MWNTs-$(NH_2)_n$. The MWNT-*g*-$(PBLG)_n$ was soluble in strong polar solvents, such as DMF and dimethyl sulfoxide, and insoluble in weak polar solvents, such as acetone and esters.

Poly(L-lysine) is a biocompatible and biodegradable polymer, and its structure facilitates various modifications, including conjugation with transferrin, epidermal growth factor, and fusogenic peptides, and thus has been widely used in the field of gene and drug delivery. Surface-initiated ROP of ε-(benzyloxycarbonyl)-L-lysine N-carboxyanhydride used the amine groups of the functionalized MWNTs and resulted in MWNT-*g*-PLys(Z) [58]. Acidolysis of the benzyl carbamate groups afforded water-soluble MWNT-*g*-PLL. Core-shell structures were determined by high-resolution TEM with the polymer shell thickness varying between 4 and 18 nm. The heterogeneous coverage of the polymer is resulting from the random distribution of amine groups on the MWNT walls. A thicker polymer layer was observed at the bends and tips than at the straight sections.

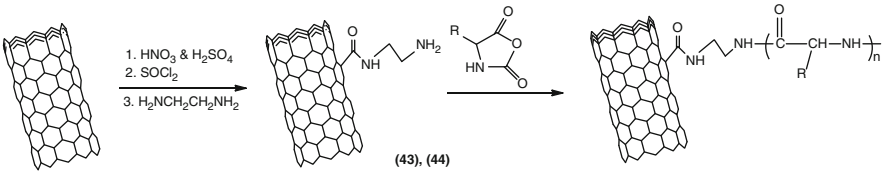

Scheme 12 Surface-initiated ROP of γ-benzyl-L-glutamate from MWNTs (Reproduced with permission from Ref. [77], Copyright 2013 RSC)

A more detailed work involving the surface-initiated ROP of BLG-NCA from amine-functionalized SWNTs revealed that chemically grafted PBLG adopted a random-coil conformation in contrast to the physically adsorbed PBLG, which exhibits an α-helical conformation [59]. It appears that intermolecular interactions of the grafted chains anchored at the one end are not favoring the helical conformation. Microfibers of PBLG nanocomposite containing SWNT-*g*-PBLG were prepared by electrospinning. Wide-angle X-ray scattering diffractograms suggested the SWNTs-*g*-PBLG were evenly distributed among PBLG rods in the solution and in the solid state, where PBLGs formed a short-range nematic phase inter-dispersed with amorphous domain.

Anionic ROP was used by Qu et al. [60] to functionalize SWNTs with nylon 6. Nylon 6 is an important commodity polymer used in a wide variety of applications. Thus, the synthesis of nylon-functionalized carbon nanotubes is expected to improve mechanical properties. ε-Caprolactam was covalently attached to the surface of the SWNTs. The monomer-grafted SWNTs were used for the polymerization of the same monomer in bulk to grow nylon 6. The nylon 6-grafted SWNTs, SWNTs-*g*-nylon 6, contained approximately 30 wt % polymer and were soluble in some organic solvents, such as formic acid and *m*-cresol (Table 1, entry 35).

The covalent functionalization of MWNTs with nylon 6 was also reported by Adronov et al. [61]. Isocyanate-functionalized CNTs, prepared by reacting MWNTs-$(OH)_n$ with excess of toluene 2,4-diisocyanate, were used as an initiator in anionic ROP of ε-caprolactam, in the presence of a sodium caprolactamate catalyst. A series of polymerizations was performed in order to investigate the effect of the reaction time and of the feed ratio (monomer/MWNT initiator) on the grafting efficiency (f_{wt} %). The results indicated an increase of the f_{wt} % with polymerization time, reaching a limiting value after 6 h and only roughly controlled by adjusting the monomer to the initiator feed ratio within the range between 150 and 800.

Polyamide 6 (PA6) was grafted from MWNTs by Yan et al. [62] in a two-step process. Initially, MWNTs were covalently functionalized with copolymer (styrene-maleic anhydride) (SMA). In the second step, in situ anionic ROP was used for the polymerization of ε-caprolactam activated by the maleic anhydride groups from the grafted polymer on the MWNTs. The MWNT-*g*-PA6 was homogeneously dispersible in organic solvents such as formic acid and could melt when mixed with ε-caprolactam. In a related study, by the same group, a similar grafting was performed using toluene 2,4-diisocyanate (TDI)-functionalized MWNTs [63].

3.4 Anionic Polymerization from Cross-Linked PS

Other than carbon materials, insoluble plastics, such as cross-linked PS beads, also represent a main category of organic support. Anionic SIP on this platform has been studied mainly by Endo and co-workers from Japan. Specifically, the authors first attached 2-bromoisobutyrate moiety by the condensation of 2-bromoisobutyric acid

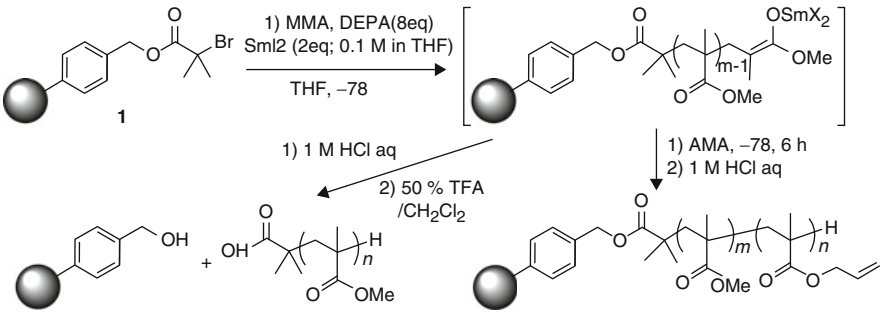

Scheme 13 Samarium (III) enolate formation and living anionic polymerization of methacrylate monomers (Reproduced with permission from Ref. [64], Copyright 2000 RSC)

with cross-linked polystyrene containing hydroxymethyl groups. Afterward, MMA anionic polymerization was initiated by samarium(III) enolate, which was generated in situ by the reduction of the corresponding bromoisobutyrate moiety using divalent samarium iodide (SmI_2). It was also demonstrated that the SIP is living, as shown by the successful block copolymerization of a second type of methacrylate (Scheme 13) [64]. Later, the same technique was extended to allyl methacrylate [65] and hydroxyethyl methacrylate [66].

4 Conclusion

Surface modification of organic and inorganic substrates using polymer grafting is critical for the development of the interface-integrated devices (sensors and actuators), self-assembly patterning, and nanocomposites in various technologies. Among several controlled polymerization techniques used for the surface-initiated polymerization from nanomaterials, living anionic polymerization has great advantages over the control of the molecular weight, the distribution, and the conformation of the polymer brushes. Although results reported so far, in several publications, indicate that obtaining predetermined graft-length and graft-density via surface-initiated anionic polymerization is very complex, it is possible to have a correction of experimental condition and these parameters for a particular system. The complexity arises from factors such as surface impurities, variations in initiator/co-initiator attachment and activation efficiencies, and the heterogeneous reaction with a wide distribution of nanomaterial's shapes and sizes.

More importantly, the efficiency of formation and the reactivity of ion-pairs in closely packed self-assembled monolayer anions on a flat substrate appear to be low as indicated by the grafting of one PS chain in 18 molecules of SAM initiator. Research in this area so far indicates a significant progress toward understanding of surface grafting and exhibits a feasibility of surface modification of nanomaterials using living anionic polymerization. However, it requires further fundamental

understanding of the efficacy and the properties of quasi-two-dimensional ionic interface-mediated polymerization for constructing precisely controlled surfaces.

Abbreviations

2VP	2-Vinylpyridine
AFM	Atomic force microscopy
AMA	Allyl methacrylate
APA	3-Azidopropan-1-amine
ATRP	Atom transfer radical polymerization
BCB-EO	4-Hydroxyethyl benzocyclobutene
BCB-PE	1-Benzocylcobutene-1′-phenylethylene
BD	Butadiene
BIBA	2-Bromoisobutyric acid
BMBP	4′-Bromo-4-mercaptobiphenyl
BuLi	*sec*-Butyl lithium
BuOLi	Lithium *tert*-butoxide
CMS	Chloromethylstyrene
CNTs	Carbon nanotubes
CoMoCAT	Co-Mo catalyst
CPC	Conductive polymer composite
CP-TES	(3-Chloropropyl)triethoxysilane
$CpTiCl_3$	Cyclopentadienyltitanium(IV) trichloride
d	Density
DAH	1,6-Diaminohexane
DCB	Dichlorobenzene
DEPA	*N*,*N*-diethylphenylacetamide
DMAEMA	2-(Dimethylamino)ethylmethacrylate
DMF	Dimethoxyethylene
DPE	1,1′-Diphenylethylene
DSC	Differential scanning calorimetry
ε-Boc-$_L$-Lys-NCA	ε-(Benzyloxycarbonyl)-$_L$-lysine *N*-carboxyanhydride
ε-CL	ε-Caprolactam
EDA	Ethylene diamine
EG	Ethylene glycol
EO	Ethylene oxide
FT	Film thicknesses
FTIR	Fourier transform infrared
GNRs	Graphene nanoribbons
GO	Graphene oxide
HEMA	Hydroxyethyl methacrylate
HPG	Hyperbranched polyglycerol
I	Isoprene

$_{L}$-LA	$_{L}$-Lactide
MA	Maleic anhydride
MDI	4,4′-Methylenebis(phenyl isocyanate)
MeOH	Methanol
MeOK	Potassium methoxide
MeONa	Sodium methoxide
MMA	Methyl methacrylate
MWD	Molecular weight distribution
MWNT	Multiwalled carbon nanotubes
NaCL	ε-Caprolactam sodium salt
NCA	N-carboxyanhydride
NMR	Nuclear magnetic resonance
NMR	Nuclear magnetic resonance
NMRP	Nitroxide-mediated radical polymerization
PA6	Polyamide 6
PBLG	Poly(γ-benzyl-$_{L}$-glutamate)
PCL	Poly(ε-caprolactam)
PEO	Poly(ethylene oxide)
PI	Polyisoprene
PLLA	Poly($_{L}$-lactide)
PMMA	Poly(methyl methacrylate)
PPDX	Poly(*p*-dioxanone)
PS	Polystyrene
PVP	Poly(2-vinyl pyridine)
RAFT	Reversible addition fragmentation chain transfer polymerization
ROP	Ring-opening polymerization
RT	Room temperature
S	Styrene
SAM	Self-assembled monolayer
SEC	Size exclusion chromatography
SIAP	Surface-initiated anionic polymerization
SIP	Surface-initiated polymerization
SmI_2	Samarium(II) iodide
$Sn(Oct)_2$	Tin(II) 2-ethylhexanoate
SWNT	Single-walled carbon nanotubes
t-BA	*tert*-Butyl acrylate
TEM	Transmission electron microscopy
TGA	Thermal gravimetric analysis
THF	Tetrahydrofuran
TMEDA	Tetramethylethylenediamine
XPS	X-ray photoelectron spectroscopy
α-CDs	α-Cyclodextrins
γ-BLG-NCA	γ-Benzyl-$_{L}$-glutamate *N*-carboxyanhydride

References

1. (a) Staudinger H (1920) Über polymerisation. Ber Deut Chem Ges 53(6):1073. doi:10.1002/cber.19200530627; (b) Paul JF (1953) Principles of polymer chemistry. Cornell University Press, USA; (c) Ajayan PM, Schadler LS, Braun PV (2003) Nanocomposite science and technology, Wiley, Weinheim
2. Hussain F, Hojjati M, Okamoto M, Gorga RE (2006) Review article: polymer-matrix nanocomposites, processing, manufacturing, and application: an overview. J Compos Mater 40(17):1511–1575. doi:10.1177/0021998306067321
3. Paul DR, Robeson LM (2008) Polymer nanotechnology: nanocomposites. Polymer 49(15):3187–3204. doi:10.1016/j.polymer.2008.04.017
4. Munch E, Launey ME, Alsem DH, Saiz E, Tomsia AP, Ritchie RO (2008) Tough, bio-inspired hybrid materials. Science 322(5907):1516–1520. doi:10.1126/science.1164865
5. Tang ZY, Kotov NA, Magonov S, Ozturk B (2003) Nanostructured artificial nacre. Nat Mater 2(6):413–U418. doi:10.1038/nmat906
6. Kuilla T, Bhadra S, Yao DH, Kim NH, Bose S, Lee JH (2010) Recent advances in graphene based polymer composites. Prog Polym Sci 35(11):1350–1375. doi:10.1016/j.progpolymsci.2010.07.005
7. Moniruzzaman M, Winey KI (2006) Polymer nanocomposites containing carbon nanotubes. Macromolecules 39(16):5194–5205. doi:10.1021/ma060733p
8. Thostenson ET, Ren ZF, Chou TW (2001) Advances in the science and technology of carbon nanotubes and their composites: a review. Compos Sci Technol 61(13):1899–1912. doi:10.1016/s0266-3538(01)00094-x
9. Giannelis EP (1996) Polymer layered silicate nanocomposites. Adv Mater 8(1):29–35. doi:10.1002/adma.19960080104
10. Ajayan PM, Schadler LS, Giannaris C, Rubio A (2000) Single-walled carbon nanotube-polymer composites: strength and weakness. Adv Mater 12(10):750–753. doi:10.1002/(sici)1521-4095(200005)12:10<750::aid-adma750>3.0.co;2-6
11. Wittmer JP, Cates ME, Johner A, Turner MS (1996) Diffusive growth of a polymer layer by in situ polymerization. Europhys Lett 33(5):397–402. doi:10.1209/epl/i1996-00347-0
12. Advincula R (2006) Polymer brushes by anionic and cationic Surface-Initiated Polymerization (SIP). In: Jordan R (ed) Surface-initiated polymerization I, vol 197, Advances in polymer science. Springer, Berlin, pp 107–136. doi:10.1007/12_066
13. Zhou Q, Nakamura Y, Inaoka S, Park M, Wang Y, Mays J (2002) In: Krishnamoorti R, Vaia R A (eds) Polymer nanocomposites. ACS symposium series No 804. American Chemical Society, Washington, DC
14. Zhou QY, Fan XW, Xia CJ, Mays J, Advincula R (2001) Living anionic surface initiated polymerization (SIP) of styrene from clay surfaces. Chem Mater 13(8):2465–2467. doi:10.1021/cm0101780
15. Quirk RP, Mathers RT (2001) Surface-initiated living anionic polymerization of isoprene using a 1,1-diphenylethylene derivative and functionalization with ethylene oxide. Polym Bull (Berlin) 45:471–477. doi:10.1007/s002890170100
16. Advincula R, Zhou Q, Mays J (2001) Nanocomposite materials by surface initiated polymerization on silicate, clay, and Si-gel surfaces: Preparation of high performance barrier materials. Polym Mater Sci Eng 84:875
17. Quirk RP, Mathers RT (2001) Surface grafting to and from 1,1-diphenylethylene using a surface-bound monolayer and functionalization of the living chain ends with ethylene oxide. Polym Mater Sci Eng 84:873
18. Quirk RP, Mathers RT (2001) Surface grafted poly(isoprene-block-ethylene oxide) diblock copolymer brushes from a 1,1-diphenylethylene surface-bound monolayer. Polym Mater Sci Eng 85:198
19. Zhou Q, Fan X, Xia C, Mays J, Advincula R (2001) Anionic polymerization initiated from Si-gel and clay nanoparticle surfaces. Polym Mater Sci Eng 84:835

20. Zhou Q, Nakamura Y, Inaoka S, Park M, Wang Y, Mays J, Advincula R (2000) Surface initiated anionic polymerization on silica and silicate surfaces. Polym Mater Sci Eng 82:290
21. Zhou Q, Wang S, Fan X, Mays J, Advincula R, Sakellariou G, Pispas S, Hadjichristides N (2001) Nanocomposite materials prepared by surface initiated anionic polymerization from Si-gel and clay nanoparticle surfaces: homopolymers and block-copolymers. Polym Prepr (Am Chem Soc Div Polym Chem) 42:59
22. Quirk RP, Mathers RT, Cregger T, Foster MD (2002) Anionic synthesis of block copolymer brushes grafted from a 1,1-diphenylethylene monolayer. Macromolecules 35(27):9964–9974. doi:10.1021/ma011536n
23. Baskaran D, Sivaram S (1997) Specific salt effect of lithium perchlorate in living anionic polymerization of methyl methacrylate and *tert*-butyl acrylate. Macromolecules 30(6): 1550–1555. doi:10.1021/ma961118w
24. Wiles DM, Bywater S (1965) Polymerization of methyl methacrylate initiated by 1,1-diphenylhexyl lithium. Trans Faraday Soc 61(505P):150–158. doi:10.1039/tf9656100150
25. Jordan R, Ulman A, Kang JF, Rafailovich MH, Sokolov J (1999) Surface-initiated anionic polymerization of styrene by means of self-assembled monolayers. J Am Chem Soc 121(5):1016–1022. doi:10.1021/ja9813481
26. Milner ST, Witten TA, Cates ME (1988) Theory of the grafted polymer brush. Macromolecules 21(8):2610–2619. doi:10.1021/ma00186a051
27. Sakellariou G, Park M, Advincula R, Mays JW, Hadjichristidis N (2006) Homopolymer and block copolymer brushes on gold by living anionic surface-initiated polymerization in a polar solvent. J Polym Sci Polym Chem 44(2):769–782. doi:10.1002/pola.21195
28. Fan XW, Zhou QY, Xia CJ, Cristofoli W, Mays J, Advincula R (2002) Living anionic surface-initiated polymerization (LASIP) of styrene from clay nanoparticles using surface bound 1,1-diphenylethylene (DPE) initiators. Langmuir 18(11):4511–4518. doi:10.1021/la025556+
29. Oosterling M, Sein A, Schouten AJ (1992) Anionic grafting of polystyrene and poly(styrene-block-isoprene) onto microparticulate silica and glass slides. Polymer 33(20):4394–4400. doi:10.1016/0032-3861(92)90286-6
30. Zhou QY, Wang SX, Fan XW, Advincula R, Mays J (2002) Living anionic surface-initiated polymerization (LASIP) of a polymer on silica nanoparticles. Langmuir 18(8):3324–3331. doi:10.1021/la015670c
31. Advincula R, Zhou QG, Park M, Wang SG, Mays J, Sakellariou G, Pispas S, Hadjichristidis N (2002) Polymer brushes by living anionic surface initiated polymerization on flat silicon (SiO (x)) and gold surfaces: homopolymers and block copolymers. Langmuir 18(22):8672–8684. doi:10.1021/la025962t
32. Kim CJ, Sondergeld K, Mazurowski M, Gallei M, Rehahn M, Spehr T, Frielinghaus H, Stuhn B (2013) Synthesis and characterization of polystyrene chains on the surface of silica nanoparticles: comparison of SANS, SAXS, and DLS results. Colloid Polym Sci 291(9): 2087–2099. doi:10.1007/s00396-013-2923-z
33. Khan M, Huck WTS (2003) Hyperbranched polyglycidol on Si/SiO2 surfaces via surface-initiated polymerization. Macromolecules 36(14):5088–5093. doi:10.1021/ma0340762
34. Tsubokawa N, Yoshihara T, Sone Y (1992) Grafting of polymers onto carbon whisker by anionic graft-polymerization of vinyl monomers using metallized aromatic rings and or phenoxy lithium groups on the surface as initiator. J Polym Sci A Polym Chem 30(4): 561–567. doi:10.1002/pola.1992.080300406
35. Lu W, Ruan GD, Genorio B, Zhu Y, Novosel B, Peng ZW, Tour JM (2013) Functionalized graphene nanoribbons via anionic polymerization initiated by alkali metal-intercalated carbon nanotubes. ACS Nano 7(3):2669–2675. doi:10.1021/nn400054t
36. Zhang XQ, Fan XY, Li HZ, Yan C (2012) Facile preparation route for graphene oxide reinforced polyamide 6 composites via in situ anionic ring-opening polymerization. J Mater Chem 22(45):24081–24091. doi:10.1039/c2jm34243j

37. Viswanathan G, Chakrapani N, Yang HC, Wei BQ, Chung HS, Cho KW, Ryu CY, Ajayan PM (2003) Single-step in situ synthesis of polymer-grafted single-wall nanotube composites. J Am Chem Soc 125(31):9258–9259. doi:10.1021/ja0354418
38. Chen SM, Chen DY, Wu GZ (2006) Grafting of poly(*t*BA) and P*t*BA-b-PMMA onto the surface of SWNTs using carbanions as the initiator. Macromol Rapid Commun 27(11): 882–887. doi:10.1002/marc.200600049
39. Liang F, Beach JM, Kobashi K, Sadana AK, Vega-Cantu YI, Tour JM, Billups WE (2006) In situ polymerization initiated by single-walled carbon nanotube salts. Chem Mater 18(20): 4764–4767. doi:10.1021/cm0607536
40. Sakellariou G, Ji HN, Mays JW, Baskaran D (2008) Enhanced polymer grafting from multiwalled carbon nanotubes through living anionic surface-initiated polymerization. Chem Mater 20(19):6217–6230. doi:10.1021/cm801449t
41. Yoon KR, Kim WJ, Choi IS (2004) Functionalization of shortened single-walled carbon nanotubes with poly (p-dioxanone) by 'Grafting-From' approach. Macromol Chem Phys 205(9):1218–1221. doi:10.1002/macp.200400077
42. Zhou L, Gao C, Xu WJ (2009) Efficient grafting of hyperbranched polyglycerol from hydroxyl-functionalized multiwalled carbon nanotubes by surface-initiated anionic ring-opening polymerization. Macromol Chem Phys 210(12):1011–1018. doi:10.1002/macp.200900134
43. Adeli M, Mirab N, Alavidjeh MS, Sobhani Z, Atyabi F (2009) Carbon nanotubes-graft-polyglycerol: biocompatible hybrid materials for nanomedicine. Polymer 50(15):3528–3536. doi:10.1016/j.polymer.2009.05.052
44. Buffa F, Hu H, Resasco DE (2005) Side-wall functionalization of single-walled carbon nanotubes with 4-hydroxymethylaniline followed by polymerization of epsilon-caprolactone. Macromolecules 38(20):8258–8263. doi:10.1021/ma050876w
45. Zeng HL, Gao C, Yan DY (2006) Poly(epsilon-caprolactone)-functionalized carbon nanotubes and their biodegradation properties. Adv Funct Mater 16(6):812–818. doi:10.1002/adfm.200500607
46. Castro M, Lu J, Bruzaud S, Kumar B, Feller J-F (2009) Carbon nanotubes/poly(epsilon-caprolactone) composite vapour sensors. Carbon 47(8):1930–1942. doi:10.1016/j.carbon.2009.03.037
47. Ruelle B, Peeterbroeck S, Gouttebaron R, Godfroid T, Monteverde F, Dauchot J-P, Alexandre M, Hecq M, Dubois P (2007) Functionalization of carbon nanotubes by atomic nitrogen formed in a microwave plasma Ar + N-2 and subsequent poly(epsilon-caprolactone) grafting. J Mater Chem 17(2):157–159. doi:10.1039/b613581c
48. Yang Y, Tsui CP, Tang CY, Qiu S, Zhao Q, Cheng X, Sun Z, Li RKY, Xie X (2010) Functionalization of carbon nanotubes with biodegradable supramolecular polypseudorotaxanes from grafted-poly(epsilon-caprolactone) and alpha-cyclodextrins. Eur Polym J 46(2):145–155. doi:10.1016/j.eurpolymj.2009.10.020
49. Priftis D, Sakellariou G, Hadjichristidis N, Penott EK, Lorenzo AT, Muller AJ (2009) Surface modification of multiwalled carbon nanotubes with biocompatible polymers via ring opening and living anionic surface initiated polymerization. Kinetics and crystallization behavior. J Polym Sci Polym Chem 47(17):4379–4390. doi:10.1002/pola.23491
50. Priftis D, Sakellariou G, Mays JW, Hadjichristidis N (2010) Novel diblock copolymer-grafted multiwalled carbon nanotubes via a combination of living and controlled/living surface polymerizations. J Polym Sci Polym Chem 48(5):1104–1112. doi:10.1002/pola.23865
51. Chen G-X, Kim H-S, Park B-H, Yoon J-S (2007) Synthesis of poly(L-lactide)-functionalized multiwalled carbon nanotubes by ring-opening polymerization. Macromol Chem Phys 208 (4):389–398. doi:10.1002/macp.200600411
52. Kim H-S, Park B-H, Yoon J-S, Jin H-J (2007) Thermal and electrical properties of poly (L-lactide)-graft-multiwalled carbon nanotube composites. Eur Polym J 43(5):1729–1735. doi:10.1016/j.eurpolymj.2007.02.025

53. Kim H-S, Chae Y-S, Park B-H, Yoon J-S, Kang M-S, Jin H-J (2008) Thermal and electrical conductivity of poly(L-lactide)/multiwalled carbon nanotube nanocomposites. Curr Appl Phys 8(6):803–806. doi:10.1016/j.cap.2007.04.032
54. Priftis D, Petzetakis N, Sakellariou G, Pitsikalis M, Baskaran D, Mays JW, Hadjichristidis N (2009) Surface-initiated titanium-mediated coordination polymerization from catalyst-functionalized single and multiwalled carbon nanotubes. Macromolecules 42(9):3340–3346. doi:10.1021/ma8027479
55. Chakoli AN, Wan J, Feng J, Amirian M, Sui J, Cai W (2009) Functionalization of multiwalled carbon nanotubes for reinforcing of poly(L-lactide-co-epsilon-caprolactone) biodegradable copolymers. Appl Surf Sci 256(1):170–177. doi:10.1016/j.apsusc.2009.07.103
56. Feng J, Cai W, Sui J, Li Z, Wan J, Chakoli AN (2008) Poly(L-lactide) brushes on magnetic multiwalled carbon nanotubes by in-situ ring-opening polymerization. Polymer 49(23): 4989–4994. doi:10.1016/j.polymer.2008.09.022
57. Yao Y, Li W, Wang S, Yan D, Chen X (2006) Polypeptide modification of multiwalled carbon nanotubes by a graft-from approach. Macromol Rapid Commun 27(23):2019–2025. doi:10.1002/marc.200600447
58. Li J, He W, Yang L, Sun X, Hua Q (2007) Preparation of multi-walled carbon nanotubes grafted with synthetic poly(L-lysine) through surface-initiated ring-opening polymerization. Polymer 48(15):4352–4360. doi:10.1016/j.polymer.2007.05.076
59. Tang H, Zhang D (2010) Poly(gamma-benzyl-l-glutamate)-functionalized single-walled carbon nanotubes from surface-initiated ring-opening polymerizations of N-carboxylanhydride. J Polym Sci Pol Chem 48(11):2340–2350. doi:10.1002/pola.24001
60. Qu LW, Veca LM, Lin Y, Kitaygorodskiy A, Chen BL, McCall AM, Connell JW, Sun YP (2005) Soluble nylon-functionalized carbon nanotubes from anionic ring-opening polymerization from nanotube surface. Macromolecules 38(24):10328–10331. doi:10.1021/ma051762n
61. Yang M, Gao Y, Li H, Adronov A (2007) Functionalization of multiwalled carbon nanotubes with polyamide 6 by anionic ring-opening polymerization. Carbon 45(12):2327–2333. doi:10.1016/j.carboji.2007.07.021
62. Yan D, Yang G (2009) A novel approach of in situ grafting polyamide 6 to the surface of multi-walled carbon nanotubes. Mater Lett 63(2):298–300. doi:10.1016/j.matlet.2008.10.013
63. Yan D, Yang G (2009) Synthesis and properties of homogeneously dispersed polyamide 6/mwnts nanocomposites via simultaneous in situ anionic ring-opening polymerization and compatibilization. J Appl Polym Sci 112(6):3620–3626. doi:10.1002/app.29783
64. Tanaka M, Sudo A, Sanda F, Endo T (2000) Samarium enolate on crosslinked polystyrene beads: anionic initiator for well defined synthesis of polymethacrylate on a solid support. Chem Commun 24:2503–2504. doi:10.1039/b007259l
65. Tanaka M, Sudo A, Sanda F, Endo T (2003) Samarium enolate on crosslinked polystyrene beads. II. An anionic initiator for the well-defined synthesis of poly(allyl methacrylate) on a solid support. J Polym Sci Polym Chem 41(6):853–860. doi:10.1002/pola.10626
66. Tanaka M, Sudo A, Endo T (2004) Samarium enolate on crosslinked polystyrene beads. III. Anionic initiator for well-defined synthesis of poly(hydroxyethyl methacrylate) on solid support. J Polym Sci Polym Chem 42(17):4417–4423. doi:10.1002/pola.20210
67. Minoura Y, Katano M (1969) Graft copolymerization of styrene with carbon black-alkali metal complex. J Appl Polym Sci 13 (10):2057–2068. doi:10.1002/app.1969.070131003
68. Ohkita K, Nakayama N, Shimomura M (1980) The polymerization of styrene catalyzed by normal-butyllithium in the presence of carbon-black. Carbon 18(4):277–280. doi:10.1016/0008-6223(80)90051-2
69. Tsubokawa N, Funaki A, Hada Y, Sone Y (1982) Grafting polyesters onto carbon-black. I. Polymerization of beta-propiolactone initiated by alkali-metal carboxylate group on the surface of carbon-black. J Polym Sci Polym Chem 20(12):3297–3304. doi:10.1002/pol.1982.170201204

70. Dresselhaus MS, Dresselhaus G (2002) Intercalation compounds of graphite. Adv Phys 51(1):1–186. doi:10.1080/00018730110113644
71. Geim AK, Novoselov KS (2007) The rise of graphene. Nat Mater 6(3):183–191. doi:10.1038/nmat1849
72. Stein C, Gole J (1966) Anionic polymerization of dienes under the effect of insertion products of alkaline metals into graphite. Bull Soc Chim Fr 10:3175–3181
73. Leroux F, Besse JP (2001) Polymer interleaved layered double hydroxide: a new emerging class of nanocomposites. Chem Mater 13(10):3507–3515. doi:10.1021/cm0110268
74. Sun LY, Xiao M, Liu JJ, Gong K (2006) A study of the polymerization of styrene initiated by K-THF-GIC system. Eur Polym J 42(2):259–264. doi:10.1016/j.eurpolymj.2005.07.014
75. Barbey R, Lavanant L, Paripovic D, Schuwer N, Sugnaux C, Tugulu S, Klok HA (2009) Polymer brushes via surface-initiated controlled radical polymerization: synthesis, characterization, properties, and applications. Chem Rev 109(11):5437–5527. doi:10.1021/cr900045a
76. Pyun J, Kowalewski T, Matyjaszewski K (2003) Synthesis of polymer brushes using atom transfer radical polymerization. Macromol Rapid Commun 24(18):1043–1059. doi:10.1002/marc.200300078
77. Sakellariou G, Priftis D, Baskaran D (2013) Surface-initiated polymerization from carbon nanotubes: strategies and perspectives. Chem Soc Rev 42(2):677–704. doi:10.1039/c2cs35226e
78. Baskaran D, Mays JW, Bratcher MS (2004) Polymer-grafted multiwalled carbon nanotubes through surface-initiated polymerization. Angew Chem Int Edit 43(16):2138–2142. doi:10.1002/anie.200353329
79. Edmondson S, Osborne VL, Huck WTS (2004) Polymer brushes via surface-initiated polymerizations. Chem Soc Rev 33(1):14–22. doi:10.1039/b210143m
80. Hadjichristidis N, Pitsikalis M, Pispas S, Iatrou H (2001) Polymers with complex architecture by living anionic polymerization. Chem Rev 101(12):3747–3792. doi:10.1021/cr9901337
81. Baskaran D, Sakellariou G, Mays JW, Bratcher MS (2007) Grafting reactions of living macroanions with multi-walled carbon nanotubes. J Nanosci Nanotechnol 7(4–5):1560–1567. doi:10.1166/jnn.2007.459
82. Sakellariou G, Ji H, Mays JW, Hadjichristidis N, Baskaran D (2007) Controlled covalent functionalization of multiwalled carbon nanotubes using 4 + 2 cycloaddition of benzocyclobutenes. Chem Mater 19(26):6370–6372. doi:10.1021/cm702470x
83. Kamber NE, Jeong W, Waymouth RM, Pratt RC, Lohmeijer BGG, Hedrick JL (2007) Organocatalytic ring-opening polymerization. Chem Rev 107(12):5813–5840. doi:10.1021/cr068415b
84. Gao C, He H, Zhou L, Zheng X, Zhang Y (2009) Scalable functional group engineering of carbon nanotubes by improved one-step nitrene chemistry. Chem Mater 21(2):360–370. doi:10.1021/cm802704c
85. Ma J, Cheng X, Ma X, Deng S, Hu A (2010) Functionalization of multiwalled carbon nanotubes with polyesters via bergman cyclization and 'Grafting from' strategy. J Polym Sci Polym Chem 48(23):5541–5548. doi:10.1002/pola.24365
86. Lee R-S, Chen W-H, Lin J-H (2011) Polymer-grafted multi-walled carbon nanotubes through surface-initiated ring-opening polymerization and click reaction. Polymer 52(10):2180–2188. doi:10.1016/j.polymer.2011.03.020
87. Chen J, Dyer MJ, Yu MF (2001) Cyclodextrin-mediated soft cutting of single-walled carbon nanotubes. J Am Chem Soc 123(25):6201–6202. doi:10.1021/ja015766t
88. Hadjichristidis N, Iatrou H, Pitsikalis M, Sakellariou G (2009) Synthesis of well-defined polypeptide-based materials via the ring-opening polymerization of alpha-amino acid N-carboxyanhydrides. Chem Rev 109(11):5528–5578. doi:10.1021/cr900049t